TECHNICAL REPORT 121-4

SUPERCAVITATING PROPELLERS – MOMENTUM THEORY

By

Marshall P. Tulin

September 1964

HYDRONAUTICS, incorporated
research in hydrodynamics

Research, consulting, and advanced engineering in the fields of NAVAL and INDUSTRIAL HYDRODYNAMICS. Offices and laboratory in the Washington, D. C. area: Pindell School Road, Howard County, Laurel, Md.

HYDRONAUTICS, Incorporated

TECHNICAL REPORT 121-4

SUPERCAVITATING PROPELLERS — MOMENTUM THEORY

By

Marshall P. Tulin

September 1964

Supported Under

Contract Nonr-3435(00)
Office of Naval Research
Navy Department

TABLE OF CONTENTS

NOTATION

A_o	Closed tunnel cross-section area
A_1	Area of circle circumscribing the propeller (disc area)
A_{2_o}	Transverse area of downstream flow outside of choked propeller slipstream
A_{2_j}	Transverse area of downstream flow in jets within choked propeller slipstream
A_3	Transverse area of propeller slipstream at region of cavity collapse
C_D	Drag coefficient of drag disc based on the disc area and upstream speed
C_T	Thrust coefficient, $T/\frac{1}{2}\rho U_o^2 A_1$
D_c	Form drag on blade element due to cavitation
Δh	Stagnation pressure change across actuator disc
k_t	Thrust coefficient, $T/\rho n^2 D^4$
L	Blade element lift
p	Static pressure
T	Thrust
U	Flow speed
U_c	Flow speed corresponding to cavitating conditions
η	Propeller efficiency
η_i	Propeller induced efficiency (also U_o/U_1)
η_c	Propeller or blade cavitational efficiency (See Equation [7])

λ_e	Advance ratio (axial inflow speed/blade relative rotational speed)
ρ	Fluid density

Subscripts o, 1, 2, 3 and 4 when used in connection with p, U and η refer to conditions at the corresponding planes transverse to the flow:

- o - far upstream
- 1 - just upstream of the propeller disc
- 2 - through the maximum section of the cavity
- 3 - just downstream of the cavity collapse
- 4 - far downstream

The subscript max refers to the maximum allowable value.

LIST OF FIGURES

INTRODUCTION

The supercavitating propeller was introduced into marine technology by Soviet Acadamician V. L. Posdunine, References 1, 2, and 3. Later, research at the David Taylor Model Basin, particularly on the subject of efficient supercavitating blade sections, led to the adoption in Western Countries of supercavitating propellers for high speed planing craft and hydrofoil boats, References 4 - 7. The use of such propellers is expanding at the present time and with the increase in size and speeds of contemplated hydrofoil craft they would seem to play an increasingly more important role in marine technology. In an earlier paper, Reference 8 the author has discussed the history, operating characteristics, and mechanism of operation of supercavitating propellers. The present paper may be regarded as a companion to this earlier work.

Our understanding of the hydrodynamics of supercavitating propellers is quite imperfect. We have not quantitatively understood well enough many aspects of their design and operation. Two hydrodynamic effects have been particularly ignored or shrouded in mystery. These are: (i) the interference between supercavitating blades and their cavities, see Reference 8, and (ii) the effect of the cavities on the inflow to the propeller. This paper is specifically devoted to the latter effect.

It is important to have accurate knowledge of the inflow speeds at the propeller disc in order that the effective angles of attack at which the blade elements operate may be calculated.

For a subcavitating propeller this inflow is generated almost entirely by the vortex wake shed behind the propeller as a consequence of its thrusting action. The inflow speed to a thrusting subcavitating propeller is always greater than the relative free-stream speed and increases with increasing thrust. A rough idea of this inflow speed may be gotten from momentum theory (Froude-Rankine); precise calculations including the actual distribution of inflow speed with radial distance from the shaft may be made using Goldstein factors, Lerbs induction factors, or other similar methods, see Reference 9 .

It has been customary in this country to assume that the inflow speed to a supercavitating propeller could be calculated exactly in the same way as for a subcavitating propeller. The effect on the inflow of the cavities shed by the blades was thereby ignored. The present paper clearly shows that for a heavily supercavitating propeller the inflow speed is actually determined largely by the blockage effects due to the shed cavities. Furthermore, it is highly probable that even under normal design conditions when the shed cavity volume is at a minimum, predictions of inflow speed which ignore the blockage effect of the shed cavities will be grossly in error.

Posdunine clearly understood the importance of cavity blockage effects for the performance of supercavitating propellers, and several Soviet papers have been devoted to the extension of the momentum theory of propellers to the supercavitating case, References 10 , 11 , and 12 . However, none of these works have produced adequate or correct results. In the first two, very restrictive and incorrect assumptions about the flow have been made.

Epshteyn, Reference 12, does in fact summarize the shortcomings of these papers. He, himself, attempts an analysis with a minimum of assumptions. His work fails for two reasons: he applies incorrectly* the energy theorem in a non-moving system of coordinates (his Equation 2.7), and he does not introduce the blade cavitational efficiency, η_c, into the analysis. In fact none of these interesting Soviet papers takes this latter step. This must be done, for without the introduction of such a parameter the problem of determining the inflow speed or the ideal propeller efficiency remains indeterminate. The blade cavitational efficiency arises naturally in the analysis because the head rise across the disc is not equal to the thrust loading as in subcavitating flow, but to the ratio of thrust loading and blade cavitational efficiency.

The primary objective of the present paper is to present an adequate theory relating the net propeller efficiency and inflow speed of an idealized heavily supercavitating propeller to the thrust coefficient, cavitation number and blade cavitational efficiency. This is done using momentum theory. The results clearly show that the inflow speed to a heavily supercavitating propeller will very often be retarded, contrary to the predictions of the

---

* His Equation [2.8] is based on the assumption that induced velocities exist only within the slipstream. This is clearly not true unless the free stream cavitation number is zero ($\sigma_o = 0$), and even in this case Epshteyn's analysis is incorrect except under those particular conditions when the asymptotic cavity diameter is finite. His results may in fact, when properly interpreted, be shown equal to ours in this latter very special case.

subcavitating propeller momentum theory. It is also shown that a maximum possible net efficiency exists for a heavily supercavitating propeller; this maximum is a function of thrust loading and cavitation number.

Further objectives of this paper are to discuss the general characteristics of the flow behind the cavity and in the slipstream behind a supercavitating propeller and drag discs and to discuss the effects of tunnel walls upon the propeller flow. This is done and it is shown that the inflow speed to a supercavitating propeller is not affected by tunnel boundaries even during operation between solid walls. However, tunnel choking can occur in the latter circumstances and the momentum theory is applied to its prediction.

THE MOMENTUM THEORY FOR SUBCAVITATING PROPELLERS

It is first of all useful to review the basis for the momentum theory of subcavitating propellers as it is understood at the present time, but not necessarily as it was originally conceived. The thickness of the propeller blades is neglected so that they may be thought of as vortex surfaces composed of continuous distributions of vortex lines. These lines must of course be continuous in the fluid, so that they are shed from the blades into the propeller wake to form there one continuous trailing helical sheet per blade. The space behind the propeller is thus to a certain extent filled by shed vorticity. The latter may at each point where it exists be vectorially decomposed into a longitudinal and circumferential component, which induce, respectively, rotational and axial velocities in the flow.

If the number of blades becomes very large and the chord of each very short, it becomes possible to represent the axial flow field due to the propeller by consideration only of the effect of the circumferential component of the shed vorticity. This vorticity, in turn, may be thought of as comprising a continuous distribution of concentric vortex sheaths. These are of a radius which contracts behind the propeller, but for light loadings this contraction may be neglected. The propeller blades themselves degenerate into a disc composed of essentially radial vortex lines. These induce equal but opposite circumferential velocities across the disc. The longitudinal shed vorticity induces angular velocities which exactly cancels out the influence of the disc at any point in front of or outside the propeller slipstream, where the flow, in view of its irrotationality, cannot possess angular momentum. The angular velocities just behind the disc are thus half due to the longitudinal component of shed vorticity and half due to the bound vorticity in the disc. The increase in angular momentum at any point across the disc is in reaction to and linearly related to the local torque on the blade system.

Simple momentum theories incorporate the axial flow system as described above plus an assumed discontinuity in flow stagnation pressure across the disc, but neglects the rotational flow in the slipstream. This is a consistent procedure in the case of the usual subcavitating propeller for the following reasons. When viewed in a system rotating with the propeller, a static pressure increase is caused across the disc proportional to the difference in the squares of the circumferential velocities and less the head loss due to frictional dissipation at the disc,

the other components being continuous across the disc; this static pressure increase may also be shown equal to the local net thrust loading. When neglecting the rotational component of the flow it therefore becomes necessary to account for the pressure increase across the disc in terms of an imaginary increase in the stagnation pressure of the axially symmetric flow in amount just equal to the net thrust loading. The situation is more fully discussed in the next section of this paper, with particular emphasis on the changes brought about by supercavitating operation.

Another facet of the sheath representation which is of practical and theoretical importance concerns the relation between the vortex sheath and so-called actuator or sink disc representation of the flow field. Consider a single vortex sheath of semi-infinite length, which may also be thought of as a continuous distribution of vortex rings of constant strength. This vortex sheath is exactly equivalent with regard to the flow field produced, to a sink disc just covering its open end, plus a uniform flow within the cylinder formed by the sheath and disc, Reference 13 , pg. 56. The strength of this uniform flow is such as to cause the velocity across the disc to be continuous.

Because of this equivalence, which is expressed schematically in Figure 1, it is possible in the case of light loadings to represent the flow field caused by a given axially symmetric distribution of thrust as that due to a sink disc whose radial strength depends on the loading distribution. This has been done in practice, Reference 14 . It may further be noted that a vortex sheath of finite length may be represented by tandem source-sink discs plus the contained uniform flow.

The actuator disc rather than the vortex sheath picture is usually taken as the starting point of the momentum theory. Despite the usual neglect of rotation, the idealization of the propeller action introduced in the simple actuator disc model is fair enough in portraying the propeller as a device functioning continuously to accelerate fluid aft and to do useful work as a result of the reaction on the blades and shaft. The axial flow field is asymmetric when viewed from the propeller plane by an observer moving with the speed that prevails there. This asymmetry has as a consequence that the total increase in flow momentum as observed in the wake far downstream where the pressure has returned to ambient is just twice the increase in flow momentum as observed at the propeller disc. The pressure just behind the disc is, of course, greater than ambient and therein is stored half of the momentum eventually to be delivered to the slipstream. In view of continuity the flow velocity immediately in front of the disc is identical to the velocity just aft of it, but no work having been done on those fluid elements which have yet to pass through the disc, the increased momentum of the incoming flow has been realized at the expense of the pressure, which is suitably reduced.

In the absence of blade friction or form drag, the work done on an element of the flow on passing through the disc is simply the pressure increase across the disc times the velocity of the flow at the disc, say U_1, while the useful work done by the corresponding element of the propeller is simply the net thrust loading times the absolute forward velocity of the propeller, say U_o. The net thrust loading is also just equal to the head rise

across the disc. The ideal efficiency is thus U_o/U_1. The pressure increase across the actuator disc, which equals the local net thrust loading, is also just equal to the gain in kinetic energy represented by the acceleration of the flow from far upstream to far downstream. As noted earlier, thi. pressure rise is also equal to the loss in rotational kinetic energy across the disc. These last facts allow the derivation of the result that the induced velocity at any point in the propeller disc is normal to the resultant relative velocity of a blade section.

Some important results of the simple momentum theory are presented below where some of the symbols are defined in Figure 2:

$$U_2/U_o = \sqrt{1 + C_T} \qquad [1]$$

$$U_1/U_o = \frac{1 + \sqrt{1 + C_T}}{2} \qquad [2]$$

$$\eta_i = \frac{2}{1 + \sqrt{1 + C_T}} \qquad [3]$$

The actual pressures on a rotating propeller blade vary widely from a maximum equal to the stagnation pressure based on the relative speed at the tip section to a minimum which cannot be significantly less than vapor pressure. In general, of course, the pressures on the upstream faces are lower than on the downstream sides, but the actuator disc theory in dealing with averages resulting from an idealization of the propeller thrust

distribution fails to provide significant information on the possibilities of blade cavitation. Nevertheless predictions of average pressures in the field around the propeller can be made, and are of some interest. The lowest pressures are induced immediately before the propeller disc. The pressure coefficient there decreases with increasing thrust coefficient (C_T). An upper limit to C_T, dependent on the free stream cavitation number (σ_o) is thus implied as below:

$$\frac{1 + \sqrt{1 + C_T}}{2} \leq \sqrt{1 + \sigma_o} \qquad [4]$$

and as shown in Figure 2. Of course, a propeller operating near the C_T and σ_o values implied above would be heavily supercavitating and this prediction, [4], of the usual actuator disc theory is therefore not at all correct, since cavities modify in a very important way the flow field around a supercavitating propeller. It is the main purpose of this paper to discuss such flow fields and their effect.

THE MOMENTUM THEORY FOR SUPERCAVITATING PROPELLERS

The Head Rise Across the Disc in Supercavitating Flow

Cavities originate in the plane of the supercavitating propeller and through blockage of the approaching flow cause its speed to be greater immediately behind the disc than immediately before it. These speeds, non-dimensionalized, themselves depend upon the non-dimensional thrust loading (C_T), the blade cavitation efficiency (η_c), and the free stream cavitation number (σ_o). These dependancies will be revealed later but it is first of all crucial to specify the manner in which blade cavity drag alters the relation between thrust loading and the stagnation pressure rise across the disc.

The rotation which the flow experiences upon passing through the propeller disc cannot be entirely neglected in an analysis of the propeller flow, even in the case of simple momentum theory. It has already been mentioned that when viewed in a system rotating with the propeller, a static pressure increase is caused across the disc proportional to the difference in the squares of the circumferential velocities less head losses due to friction, and that in the case of a subcavitating propeller this static pressure increase may also be shown equal to the local net thrust loading. Thus when the rotational component of the flow is "neglected" it becomes necessary to account for the head increase across the disc in terms of an imaginary increase in the stagnation pressure of the axially symmetric flow just equal to the net thrust loading (T/A_1).

In a supercavitating or separated flow, substantial cavity or form drag acts on the flow while it passes through the disc but without resulting in immediate dissipation which is assumed to occur only at the end of the cavity in the region of cavity collapse. Because the work done by the moving blades on the fluid in overcoming blade cavity drag is not dissipated at the disc, but appears there as a head rise, the net stagnation pressure increase across the disc due to flow rotation is no longer simply equal to the net thrust loading, but also depends upon the blade efficiency - to the extent that the latter reflects the blade losses due to cavity drag.

In discussing this further, it is useful to contrast again the influences of friction and form drag. The effects on the head rise across the disc of frictional blade drag and form drag such as accompanies separation or cavitation are separate and distinct. Their differing effects are the result of the dissipation which is assumed to occur at the disc accompanying frictional drag, and the absence of any such dissipation, specifically due to form drag, in the flow between the disc and the region of cavity collapse.

Thus the work done by the blades on the fluid passing through the disc in overcoming frictional drag is assumed to be not manifested at all as an increase in flow stagnation pressure-in consequence of the assumed immediate dissipation of the work input. As a result, the total increase in flow stagnation pressure across the disc in the absence of form drag (as in the usual subcavitating theory) is simply equal to the net thrust loading, and the results

of actuator disc theory apply as long as the thrust is reduced by the effect of friction drag to yield net thrust.*

However, the work input to the fluid by the blades in overcoming blade cavity drag is immediately and completely manifested in a stagnation pressure rise. The total work input to the fluid, neglecting frictional drag, is just the product of the head rise across the disc (Δh) and the volume flow through the disc ($U_1 A_1$). The useful work done by the blades on the fluid passing through the disc (considering the propeller at rest) is just the product of the net blade thrust (T) and the flow speed immediately before the propeller (U_1). If the blade cavitational efficiency (η_c) is defined as the ratio of the useful work done by the blades on the fluid passing through the disc to the work input to the blades, then:

$$\eta_c = \frac{\text{Useful Work Done on Fluid by Blades}}{\text{Total Work Input to Fluid}} = \frac{T \cdot U_1}{\Delta h \cdot U_1 A_1} \qquad [5]$$

or

$$\Delta h = \frac{T}{A_1 \cdot \eta_c} \qquad [6]$$

---

* For this reason, the potential flow calculations of propeller induced flow fields, based on blade spanwise circulation distributions uncorrected for loss of thrust due to friction, tend slightly to exaggerate these flow fields.

This result [6] is crucial in the development of a proper momentum theory for supercavitating propellers or of other propellers suffering large form drag.

The same results given above may also be obtained in a more formal manner by treating the flow in a thin annular element passing through the propeller disc as if it were the flow in a two-dimensional cascade, or by the application of an energy theorem to the flow within a proper moving control surface about the supercavitating propeller. In fact, Epshteyn in Reference 12 does apply such a theorem and [6] may be obtained from his Equation [2.4] by the substitution of TU_1/η_c for his N_3 and of A_1U_1 for his m.

The blade cavitational efficiency, η_c, is a complicated function of blade shape, effective advance coefficient, blade area ratio, and other factors. It cannot of course be calculated from momentum theory, and its accurate prediction is in fact quite difficult and outside the scope of this paper. It would seem useful, however, to state here the well-known result allowing the calculation of the local blade cavitational efficiency in terms of the cavity drag-lift ratio of the blade (D_c/L) and the effective advance ratio (λ_e).

$$\eta_c = \frac{1 - (D_c/L)(\lambda_e)}{1 + (D_c/L)(1/\lambda_e)} \qquad [7]$$

where,
$$\lambda_e = \frac{\text{Axial Inflow Speed}}{\text{Blade Relative Rotational Speed}} \qquad [8]$$

The Momentum Balance Across the Disc in Supercavitating Flow

A solid axi-symmetric obstacle producing drag in supercavitating flow sheds a cavity whose length and maximum diameter increase without bound as the cavitation number (σ_o) is reduced toward zero. In the case of a supercavitating propeller, even idealized to the actuator disc, it is not clear at the outset what the characteristics are of the trailing cavity even in the case of zero σ_o. The reason for this is that in producing thrust the propeller creates a positive pressure field behind the disc which tends to shorten the trailing cavity. We shall deduce later on that for $\sigma_o = 0$ the cavity must be infinite in length and that the diameter must also be unbounded except under certain special conditions when the asymptotic cavity diameter is finite. For $\sigma_o > 0$ the trailing cavity must of course be of finite length and of finite maximum diameter. In fact, the typical length of the cavity behind a supercavitating propeller in open water under usual operating conditions will hardly exceed one and a half propeller diameters.*

We are not in what immediately follows concerned with the detailed shape of the trailing cavity, but we have discussed it briefly in order to prevent errors in the arrangement of the

---

* It is worthwhile to note that exaggerations of these lengths may occur during testing in a water tunnel with solid walls as a result of tunnel blockage, and the cavity may at quite high cavitation numbers even extend down the entire length of the tunnel test section — a distance usually of many propeller diameters.

momentum control surfaces — as, for example, would arise should we assume that for $\sigma_o = 0$ the cavity is always of infinite length and of finite maximum diameter.

We assume that the propeller consists of a very large number of blades of very short chord. The rotation of the slipstream behind the disc is taken into account in its effect on the "effective" pressure rise across the propeller disc, as discussed earlier, but otherwise the flow is considered to be one-dimensional — as in the usual actuator disc theory. A schematic of the flow being considered, in the case of finite cavity length, is shown in Figure 3. The flow approaching the propeller is seen to be either accelerated (narrowing stream tube), or decelerated (widening stream tube) for sufficiently low thrusts in anticipation of future results. Immediately behind the disc, the stream tube is seen rapidly to widen due to the blockage effect of the cavities shed by the blades. Due to the same effect there is assumed to exist a discontinuity in the axial velocity across the disc. The cavity-wake behind the propeller plane is filled with jets or sheets of water flowing between the cavities or voids created by the blades. The pressure in the wake is constant and equal to the cavity pressure. The speed of the flow inside and on the cavity-wake is thus constant. It is, however, greater than would be the speed of the flow on a stationary cavity at the same cavitation number, since a head increase has occurred across the disc as a result of the flow rotation behind the propeller. As discussed earlier, the work done as a result of the cavity drag experienced by the blades remains in the slipstream since no dissipation of energy is assumed

to occur until the flow passes out of the cavity-wake through the region of cavity collapse at the end of the cavity.

The momentum control surface best used to determine the inflow speed U_1 is shown as a dashed line in Figure 4. It coincides with plane 1, immediately before the disc, in its intersection with the stream tube; it coincides with the outer cavity wall between the propeller disc and plane 2, and then it coincides with the latter in its intersection with the cavity-wake.

The net thrust, T, acting on the disc is:

$$T = \rho A_1 U_1 (U_2 - U_1) + A_1 (p_2 - p_1) \qquad [9]$$

where use has been made of the equality of the pressure on the outer cavity wall and that in plane 2, and where

A_1 is the disc area
p is the static pressure
Subscript 1 refers to plane 1
Subscript 2 refers to plane 2

The static pressure difference $(p_2 - p_1)$ may be evaluated making use of Bernoulli's equation and taking into account the head rise across the disc, as given by [6]. So that,

$$(p_2 - p_1) = \frac{\rho}{2} (U_1^2 - U_2^2) + \frac{T}{A_1 \cdot \eta_c} \qquad [10]$$

Combining [9] and [10] there finally results,

$$\frac{U_1}{U_o} = \frac{U_2}{U_o} - \sqrt{\frac{C_T(1-\eta_c)}{\eta_c}} \qquad [11]$$

where $C_T = \dfrac{T}{\frac{1}{2}\rho U_o^2 A_1}$

The constant speed of the flow U_2 in the cavity wake may be determined directly from Bernoulli's equation and is:

$$\frac{U_2}{U_o} = \sqrt{1 + C_T/\eta_c + \sigma_o} \qquad [12]$$

The inflow speed to the propeller thus becomes:

$$\frac{U_1}{U_o} = \sqrt{1 + \sigma_o + C_T/\eta_c} - \sqrt{C_T(1-\eta_c)/\eta_c} \qquad [13]$$

This very important result predicts what the net effect upon the inflow must be of both the accelerating action due to the propeller's trailing vortex field accompanying thrust, and the decelerating action due to the cavity-wake which accompanies blade cavity drag. The net inflow speed may, according to [13], be

greater than (acceleration) or less than (retardation) the speed U_o far ahead of the propeller, depending upon the following conditions:

$$C_T^2 + 4C_T(1-1/\eta_c + \frac{\sigma_o}{2}) + \sigma_o^2 \quad \begin{matrix} > 0 \text{ (accelerated)} \\ < 0 \text{ (retarded)} \end{matrix} \qquad [14]$$

presented graphically as Figure 5.

The effect of decreasing σ_o is always to cause a tendency toward retardation or increased retardation of the inflow, as might naturally be expected since a decrease in σ_o would surely result in a larger volume and extent of trailing cavity. The effect of increasing C_T, η_c being held constant, is not quite as straightforward since both the accelerating action of the vortex wake and the decelerating action due to cavity drag are thereby increased; the latter increases with the quantity $C_T(1-\eta_c)/\eta_c$. Figure 7 reveals, however, that for an increase in C_T up to a certain critical value (which corresponds to the dashed line in the Figure) the retardation or tendency towards it is increased, while further increases in C_T beyond the critical value causes a tendency toward or increase in the acceleration of the inflow. Clearly, a maximum must be placed on the allowable inflow speed in order to avoid cavitation in the approaching stream; this implies the existence of a maximum attainable blade efficiency, which is not shown in Figure 5 but is discussed in a later section. At any rate, the indicated tendency toward accelerated

inflow at high C_T values probably does not occur in practice since increasing C_T (higher blade loading) must almost of necessity be accompanied by decreasing η_c.

This inflow speed ratio, U_1/U_o, is just equal to the inverse of the ideal propeller efficiency as it is normally defined. It is well to see how this definition logically arises.

The total propeller efficiency η (friction is always neglected here):

$$\eta = \frac{\text{Useful Work Done by the Propeller}}{\text{Work Input to the Propeller}} \qquad [15]$$

The denominator is simply related to the blade cavitational efficiency, η_c, according to [5], so that,

$$\eta = \frac{T \cdot U_o}{T \cdot U_1} \cdot \eta_c \qquad [16]$$

or,

$$\eta = \eta_i \cdot \eta_c \qquad [17]$$

where we have defined the ideal efficiency as,

$$\eta_i = U_o/U_1 \qquad [18]$$

so that it represents the ratio of useful work done by the propeller in thrusting motion to the useful work done by the blades on the fluid, considering the propeller to be at rest and the flow in motion toward it.

In the usual subcavitating momentum theory the ideal efficiency always takes on values less than unity. In the present case, however, the inflow may be retarded, and the ideal efficiency will thus assume values in excess of unity. This should not be too disturbing, as it is well known that even subcavitating propellers operating in strong wakes (regions of retarded flow) may enjoy efficiencies greater than unity. In blocking the oncoming flow, the cavities on a supercavitating propeller create, in a sense, a wake ahead of the propeller and in this way an increase in ideal efficiency is caused at the expense of cavity drag or blade efficiency.

The total efficiency is given by:

$$\eta = \frac{\eta_c}{\sqrt{1 + \sigma_o + C_T/\eta_c} - \sqrt{C_T(1-\eta_c)/\eta_c}} \qquad [19]$$

The question naturally arises whether increasing η_c always increases the net efficiency η, since the ideal efficiency is thereby always decreased. In theory there does exist a set of values for η_c which are positive and less than unity and which maximize η. These correspond to the following relation:

$$\frac{(1-\eta_c)\eta_c}{(\eta_c - 3/4)} = \frac{C_T}{1+\sigma_o} \qquad [20]$$

which is presented graphically as Figure 6. In fact, however, these values cannot be attained since they would be accompanied by inflow speeds more than sufficient to cause cavitation in the approaching flow. For practical ranges of η_c, then, the total or net efficiency always increases with increasing η_c.

Charts of inflow speed versus thrust coefficient with blade cavitational efficiency as a parameter and for a range of cavitation numbers are given as Figures 7a - 7f ; also shown on these plots are contours of constant total efficiency. Note that in these figures, values of U_1/U_o greater than $\sqrt{1+\sigma_o}$ are not realistic, for the reason that such values correspond to inflow static pressures less than the cavity pressure, p_c. This is further to be discussed below.

The assumptions that have been made in applying momentum considerations here deserve comment. Most important of all it has been assumed that the flow in the planes 1 and 2, Figure 4 , is one-dimensional; this means that the flow velocity is assumed to have no radial components there and that the axial component is uniform within that part of the plane cut by the momentum control surface. These assumptions are probably better met by the flow in plane 2 within the cavity than by the inflow in plane 1. The existence of radial components in the inflow speed will effect the calculation of the static pressures just before the disc,

Equation [10], by a term proportional to the square of the radial velocity. The other disturbance velocities due to the propeller (axial and rotational) enter into the momentum balance at least in terms which are proportional to their first powers, (the rotational term enters through the fictitious increase in head across the disc). The neglect of the squares of the radial velocity amounts then to the neglect of a second-order term, and is best justified when the propeller is lightly loaded. The one-dimensional assumption regarding the uniformity of the axial component of velocity, pressures, etc. is of a different kind, for it does not even correspond to reality in the limiting case of a very lightly loaded propeller. The reason for this is that desirable distributions of radial loading and corresponding inflow speeds are quite non-uniform for all propeller loadings. Nevertheless, the predictions of momentum theory are highly useful in the case of subcavitating propellers when corrected for finite blade number because they may reasonably be applied separately to each annular element, the interference between elements being small. Whether the same technique may as safely be applied to a supercavitating propeller remains an open question. The predictions of the present momentum theory are thus best regarded as gross. They would seem to be very valuable in so far as they describe some of the general features of supercavitating propeller flows, but their application in design would seem hazardous. Unfortunately, no better theory exists at the present time.

The assumption of large blade number made in this theory is necessary to insure uniformity of the flow in the circumferential direction and is not therefore additive to the one-dimensional

assumption. The conditions under which reasonable circumferential flow uniformity occurs should correspond to blade loadings such that blade interference or cascade effects dominate the flow through the blades. These blade interference effects are not discussed in this report, but it is known that they dominate the operating characteristics of supercavitating propellers for values of advance coefficient somewhat higher than that corresponding to maximum k_t (σ_o being fixed). In fact, these interference effects are themselves responsible for the existence of a maximum k_t value. It seems not unlikely that blade interference effects are very important even at the design points of typical supercavitating propellers, so that inflow speeds there more likely correspond to the present theory* rather than the subcavitating predictions usually used in design which would only apply were the influence of the cavities upon the overall flow small.

An Estimate of Absolute Maximum Efficiency

The pressures in the flow approaching the propeller are less than ambient in the case where the inflow is accelerated. In no case, however, can these pressures attain values less than those on the propeller blades. We know this to be true because in a steady potential flow such as exists ahead of and around the screw when the flow is viewed from a rotating coordinate system the

---

* For this reason, there is a tendency for the loss in lift caused by blade interference to be made up at the design point by the higher blade angles of attack which result from the reduced inflow speeds.

minimum as well as the maximum pressures must occur on bounding surfaces. The momentum theory does not, however, take such considerations into account, and as a result it allows predictions of accelerated inflows which are in excess of those required to cause cavitation in the approaching flow. These excessive inflows can however be avoided if restrictions are placed upon allowable values of blade cavitational efficiencies. These efficiencies depend upon the details of the propeller configuration (pitch, blade area ratio, loading distribution, and blade section shape) and obviously cannot be estimated from momentum theory considerations. Nevertheless, the restrictions derived from momentum theory must be realistic to the extent that the real propeller flow resembles the idealized version being considered. The restrictions upon η_c allow an estimate to be made of absolute maximum net efficiency, η_{max}, as a function of C_T and σ_o, as follows.

The maximum allowable inflow velocity U_{max} just corresponds to a pressure p_c in the approaching stream, or,

$$\frac{U_{max}}{U_o} = \sqrt{1 + \sigma_o} \qquad [21]$$

Upon the assumption that $U_{max} = U_{1_{max}}$, and using [13], the following inequalitity results:

$$\sqrt{1 + \sigma_o + C_T/\eta_c} - \sqrt{C_T(1-\eta_c)/\eta_c} < \sqrt{1 + \sigma_o} \qquad [22]$$

or, after some manipulation,

$$\eta_c < \frac{1}{1 + C_T/4(1 + \sigma_o)} \qquad [23]$$

which may also be written,

$$\left(\frac{C_T}{1 + \sigma_o}\right) < \frac{4(1-\eta_c)}{\eta_c} \qquad [24]$$

The limiting values of η_c according to [23] are shown in Figure 6 and it may be seen that they are everywhere less than those values of η_c for which η_i is a theoretical maximum. This means that the limiting values of η_c (Equation [23]) must correspond to the absolute maximum net efficiencies. Thus,

$$\eta_{max} = \eta_{c_{max}} \cdot \frac{U_o}{U_{1_{max}}} \qquad [25]$$

or,

$$\eta_{max} = \frac{\sqrt{1 + \sigma_o}}{(1 + \sigma_o) + C_T/4} \qquad [26]$$

Curves for η_{max} are given as Figure 8 .

It should carefully be kept in mind that these maximum values are not necessarily attainable in practice. Estimations of actual attainable efficiency depend upon studies of the blade elements themselves, and it seems a matter of experience that actual blade cavitational efficiencies and resulting net propeller efficiencies are quite a bit less than the absolute maximum efficiencies predicted here. It would therefore be unwise to base real expectations upon the numbers implied by Figure 8 .

The Special Case of the Drag Disc

The momentum theory developed above applies not only to those cases where net thrust is developed at the disc, but also when a net drag force acts there. In fact it may apply in the special case where no net force acts on the disc, but where at the same time the blade cavitational efficiency has gone to zero.

A "pure drag" disc might consist in its simplest form of a coarse screen inserted in a stream at sufficiently low cavitation number, σ_o, so that each wire or rod composing the screen individually sheds a trailing cavity. Or it might be comprised of a number of circular rods radiating from a rotating hub and shaft. These are called "pure drag" discs because of the absence of circulation on the element comprising the disc. In general, of course, the disc might be composed of lifting elements of such poor efficiency that a net drag actually results from their operation.

No assumptions were made in the development of the momentum theory for supercavitating flows which would restrict the validity of the results to cases of positive thrust. The results therefore

apply equally to drag discs. The drag disc does not, however, do useful work but rather has work done on it. As a result the blade cavitational efficiency becomes negative. Since the thrust is negative, too, the ratio C_T/η_c which appears in [13] and other important relations, remains of the same sign as in the case of positive thrust. This is a manifestation of the fact that work is done on the rotating blades, whether they are producing thrust or drag, and that this work appears as an increase in the stagnation pressure of the flow across the disc. However, the quantities C_T and η_c do not always appear in ratio in expressions for inflow, etc. so that some differences appear between the thrust and drag cases. For example the inflow to a drag disc is always retarded, in contrast to the case of a thrust disc where it may be either accelerated or retarded. This may be shown by considering Equation [14] in a pertinent form:

$$C_D^2 - 4C_D(1-1/\eta_c + \sigma_o/2) + \sigma_o^2 \begin{matrix} > \\ < \end{matrix} \begin{matrix} 0 \quad \text{(accelerated)} \\ 0 \quad \text{(retarded)} \end{matrix} \qquad [27]$$

or,

$$(C_D - \sigma_o)^2 \begin{matrix} > \\ < \end{matrix} 4C_D\left(\frac{\eta_c - 1}{\eta_c}\right) \qquad [28]$$

The drag on the disc is very likely to follow a law which applies very well for other blunt bodies,

$$C_D = C_D(0) + \sigma_o \qquad [29]$$

so that [28] becomes,

$$C_D^2(0) \begin{matrix} > \\ < \end{matrix} \begin{matrix} \text{(accelerated)} \\ \text{(retarded)} \end{matrix} \quad 4\left[C_D(0) + \sigma_o\right] \cdot \left(\frac{\eta_c - 1}{\eta_c}\right) \qquad [30]$$

But since $C_D(0)$ must of necessity be smaller than unity, and since η_c is negative, the lower inequality must necessarily apply. The inflow to a drag disc is therefore always retarded, as one would expect intuitively.

Another clear difference between the thrust and drag discs is in the range of possible blade cavitational efficiencies, η_c, as shown below:

$$\text{THRUST DISC} \qquad 0 < \eta_c < 1.0$$

$$\text{DRAG DISC} \qquad -\infty < \eta_c < 0$$

The case where $\eta_c = -\infty$ corresponds to the stationary screen, which causes dissipation of flow energy but absorbs no work from the shaft.

The Slipstream Behind the Cavity

A wake or slipstream trails behind the cavity shed by a supercavitating propeller or drag disc. The head inside this wake is different from that in either the main stream or in the flow between the disc and the region of cavity collapse. In the present model of these flows, the heads in each of these separate regions

is assumed to be constant, and they are bound by surfaces of discontinuity. When these surfaces are stream surfaces then the discontinuity is in the nature of a vortex sheet. Therefore with one exception* the cavity shed from a disc is bounded by a vortex sheet. The wake behind the cavity is also bounded by a vortex sheet except in the case when the net axial force on the disc is null.

Far downstream when the wake pressure has returned to ambient, the wake velocity will be either greater (thrusting propeller) or less (drag disc) than the free stream speed. This wake velocity is easily estimated from a momentum balance and the head in the wake is therefore easily calculated too.

The net axial force acting on the disc is simply related to the flux in momentum across control surfaces taken far upstream and far downstream (plane 4 in Figure 4):

$$T = \rho A_1 U_1 (U_4 - U_o) \qquad [31]$$

or,

$$\frac{T}{\rho/2\ A_1 U_o^2} = 2 \frac{U_1}{U_o} \left(\frac{U_4}{U_o} - 1 \right)$$

or,

---

* In the case of a drag disc composed of non-rotating elements.

$$C_T = \frac{2}{\eta_i}\left(\frac{U_4}{U_o} - 1\right) \qquad [32]$$

Therefore,

$$\frac{U_4}{U_o} = 1 + \frac{\eta_i C_T}{2} \qquad [33]$$

The head in the wake, h_4, is:

$$h_4 - h_o = \rho/2\left[U_4^2 - U_o^2\right] \qquad [34]$$

where h_o is the ambient head. Or, making use of Equation [33]:

$$\frac{h_4 - h_o}{\rho/2\ U_o^2} = \eta_i C_T\left(1 + \frac{\eta_i C_T}{4}\right) \qquad [35]$$

This result applies equally to sub and supercavitating flows, but in the latter case η_i is always greater than in the former, C_T being fixed. We recall that the head between the propeller disc and the region of cavity collapse, h_2, is, Equation [6]:

$$\frac{h_2 - h_o}{\rho/2\ U_o^2} = \frac{C_T}{\eta_c} \qquad [36]$$

Combining [35] and [36]:

$$\frac{h_4 - h_o}{h_2 - h_o} = \eta_i \cdot \eta_c \left(1 + \frac{\eta_i C_T}{4}\right) = \eta \left(1 + \frac{\eta_i C_T}{4}\right) \qquad [37]$$

This relation also holds in the case of the drag disc, in which case η takes on negative values. From Equation [37] the loss in head which the flow suffers in passing through the region of cavity collapse may be shown to be:

$$\frac{h_2 - h_4}{\frac{1}{2}\rho U_o^2} = C_T \left[\frac{1-\eta\left(1 + \eta_i \frac{C_T}{4}\right)}{\eta_c}\right] \qquad [38]$$

The flow speed just behind the region of cavity collapse may be estimated by taking a momentum balance across the control surface labeled II in Figure 4 . Since no external f rce acts within this surface,

$$0 = \rho A_3 U_3 (U_3 - U_2) + A_3 (p_3 - p_2) \qquad [39]$$

where use has been made of the equality of the pressure on the outer cavity wall and that in plane 2, and where

A_3 is the area of the slipstream just behind cavity collapse,

Subscript 3 refers to conditions just downstream of plane 3.

The static pressure difference (p_3-p_2) may be evaluated making use of Bernoulli's equation and taking into account the loss in head which occurs across the region of cavity collapse, so that,

$$(p_3-p_2) = \rho/2(U_2^2-U_3^2) - (h_2-h_4) \qquad [40]$$

since $h_4 = h_3$.

Using Equation [38]:

$$\frac{(p_3-p_2)}{\rho/2\ U_o^2} = \left(\frac{U_2^2 - U_3^2}{U_o^2}\right) - C_T\left[\frac{1-\eta\left(1+\eta_i\ \frac{C_T}{4}\right)}{\eta_c}\right] \qquad [41]$$

and substituting in [39]:

$$2\ \frac{U_3}{U_o}\left(\frac{U_3-U_2}{U_o}\right) = C_T\left[\frac{1-\eta\left(1+\eta_i\ \frac{C_T}{4}\right)}{\eta_c}\right] - \left(\frac{U_2^2-U_3^2}{U_o^2}\right)$$

or,

$$\left(\frac{U_3-U_2}{U_o}\right)^2 = C_T\left[\frac{1-\eta\left(1+\eta_i\ \frac{C_T}{4}\right)}{\eta_c}\right] \qquad [42]$$

Finally,

$$\frac{U_3}{U_o} = \frac{U_2}{U_o} - \sqrt{\frac{C_T\left[1-\eta\left(1+\eta_i\ \frac{C_T}{4}\right)\right]}{\eta_c}} \qquad [43]$$

where $U_2/U_o = \sqrt{1 + C_T/\eta_c + \sigma_o}$ according to [12].

This may be compared with the expression for the inflow speed, Equation [11]:

$$\frac{U_1}{U_o} = \frac{U_2}{U_o} - \sqrt{\frac{C_T(1-\eta_c)}{\eta_c}}$$

The difference between outflow and inflow speeds is thus given by:

$$\frac{U_3-U_1}{U_o} = \sqrt{\frac{C_T(1-\eta_c)}{\eta_c}} - \sqrt{\frac{C_T\left[1-\eta\left(1+\eta_i\frac{C_T}{4}\right)\right]}{\eta_c}} \qquad [44]$$

In the case of retarded inflow to a propeller or a drag disc ($\eta_i > 1$ and $\eta > \eta_c$) the second term on the right is necessarily smaller than the first and the outflow speed is thus greater than the inflow. At the same time $A_3 < A_1$. This will clearly also be the case for moderate accelerated inflow speeds. Only for sufficiently large values of thrust coefficient, as given by the upper inequality in the expression below, does the situation become reversed;

$$\frac{C_T}{4} \begin{matrix} > \\ < \end{matrix} \frac{1}{\eta_i}\left(\frac{1-\eta_i}{\eta_i}\right) \qquad \begin{matrix} A_3 > A_1 \\ A_3 < A_1 \end{matrix} \qquad [45]$$

The substitution of reasonable numbers in [44] reveals that the difference between the propeller or drag disc diameter and that of the region of cavity collapse will normally not exceed 10 percent.

The results obtained here for the slipstream characteristics are reflected in Figure 3 , in which the general features of typical flows associated with supercavitating propellers and drag discs are illustrated.

The Special Case of the Infinite Length Cavity

Only when the cavitation number σ_o is zero is it possible for the trailing cavity to extend to infinity. The conditions under which this occurs may be determined by comparing the results obtained previously for the inflow velocity with those obtained under the assumption of infinite cavity length and finite asymptotic cavity diameter. In this way we will conclude that the cavity length is always infinite for $\sigma_o = 0$ while the cavity maximum diameter is unbounded except in the particular limiting case when $U_1 = U_o$. The flow is shown schematically as Figure 9. The net thrust, T, acting on the propeller is related to the momentum flux so that,

$$T = \rho A_{2_j} U_2 (U_2 - U_o) \qquad [46]$$

where use has been made of the fact that $p_2 \equiv p_o$ and where A_{2_j} is the cross-sectional area in plane 2 of the fluid jets inside the cavity.

An increase in head, Δh, occurs across the propeller disc as a result of the rotation induced by the propeller behind it. This head change is related to the propeller loading and blade cavitational efficiency by [6],

$$\Delta h = \frac{T}{A_1}\left(\frac{1}{\eta_c}\right) = \tfrac{1}{2}\rho(U_2^2 - U_o^2)$$

where use has also been made of Bernoulli's equation, and where U_2 is the axial wake velocity everywhere behind the propeller. Therefore,

$$\frac{U_2}{U_o} = \sqrt{1 + \frac{C_T}{\eta_c}} \qquad [47]$$

As a result of wasted work being done by the propeller there is a net flux of kinetic energy in the stream,

$$\text{Energy Loss} = \rho A_{2_j} U_2 \cdot \tfrac{1}{2}(U_2 - U_o)^2 \qquad [48]$$

Considering the situation as seen by an observer at rest relative to the propeller, its net efficiency, η, becomes

$$\eta = \frac{\text{Useful Work}}{\text{Useful Work + Energy Loss}} = \frac{T \cdot U_o}{T \cdot U_o + \rho A_{2_j} U_2 \dfrac{(U_2 - U_o)^2}{2}}$$

[49]

$$\eta = \frac{U_o}{(U_o + U_2)/2} \qquad [50]$$

or, using [47] and [17],

$$\eta = \eta_i \cdot \eta_c = \frac{2}{1 + \sqrt{1+C_T/\eta_c}} \qquad [51]$$

Remembering that $\eta_i = \frac{U_o}{U_1}$, there finally results for the inflow,

$$\frac{U_1}{U_o} = \frac{\eta_c}{2}\left[1 + \sqrt{1+C_T/\eta_c}\right] \qquad [52]$$

This is seen to be a different result than obtained previously, [13], without the assumption of infinite cavity length. However, these two relations, [52] and [13], do yield the same prediction of inflow speed when,

$$C_T = 4\left(\frac{1-\eta_c}{\eta_c}\right) \qquad [53]$$

and in this case $U_1 \equiv U_o$.

A reduction of thrust below the values given by [53] in reducing the positive pressure field behind the propeller, must increase the cavity growth, η_c being held constant. We are therefore led to conclude that in the case of $\sigma_o = 0$, values of thrust which lead to retarded inflow will result in unbounded cavity diameters at infinity. At the same time thrust values leading to accelerated inflows would result in cavities of finite length for $\sigma_o = 0$. However, we recall that such thrust values are not attainable as they would cause the approach flow to cavitate.

The Effect of Tunnel Boundaries

It is very important to understand the effect upon propeller performance of the water tunnel boundaries. Measured characteristics of subcavitating propellers tested between solid walls are generally corrected according to theory developed from momentum considerations, Reference 15; the same considerations show that no corrections are necessary if the screw is tested in an open or free jet on which ambient static pressures are maintained. It is assumed, of course, that the measurement of the free stream speed in the tunnel far ahead of the screw has not been affected by the latter.

It is well known that tunnel boundaries can have a serious effect upon the length of cavities trailing behind supercavitating bodies, Reference 16, pages 12-29, 12-43. Operation within a free jet tends to shorten the cavity, while operating between solid walls lengthens it. In fact, the resulting increase in length may become extreme. A cavity of infinite length will occur in a solid-walled tunnel at a cavitation number which may be

substantially greater than zero; the tunnel is then said to be choked, and operation at reduced cavitation numbers is not possible.

Thus two questions naturally present themselves concerning the operation of supercavitating propellers in water tunnels: What corrections should be made to measured propeller characteristics on account of the wall effects?; and, under what conditions of operation of a supercavitating propeller will the flow in a solid wall tunnel choke?

In order to answer the first question it need only be recalled that the control surface which was earlier used (in connection with the momentum balance from which the inflow speed was predicted), did not extend to or involve the tunnel boundaries. Therefore, the inflow speed, within the assumptions of the present analysis, is not at all affected by tunnel boundaries, whether of the solid wall or free jet type — at least up to the point where choking occurs in a solid wall tunnel. This seems at first a somewhat surprising conclusion, since the length and shape of the shed cavity is certainly subject to wall effects. However, it would appear that the requirement for constant pressure in the flow behind the propeller, together with specified thrust loading and blade cavitational efficiency, uniquely determine the inflow speed — independent of the cavity shape. Of course, recognition must be given to the possibility that the lift effectiveness and efficiency of the sections are effected by changes in overall cavity shape, so that the thrust and net efficiency of the propeller might in this way change. Momentum considerations can not, of course, comment on this latter subject. However, taking into

account blade element considerations, it seems to us that serious effects of this kind are unlikely to occur except under extreme conditions (during tunnel choking, perhaps). Indeed, the only known experiment designed to study the effect of supercavitating propeller diameter upon its measured characteristics has concluded that no effects of screw size were present within the range of sizes and operating conditions of the tests, Reference 17 .

As for choking, there exists no doubt that supercavitating propellers can choke the flow in a solid wall tunnel. I have observed this phenomenon myself during tests of a two-bladed supercavitating propeller (HYDRONAUTICS Design H3-A) at the Swedish State Shipbuilding Experimental Tank at Göteborg. The propeller diameter was .26 meters and tests were conducted between solid walls in a square test section 0.5 m × 0.5 m. From the test results, values of C_T and η_c have been estimated at which tunnel choking occurred for four different cavitation numbers (σ_o) and these are shown in Figure 10 .

Momentum considerations allow conditions for tunnel choking to be estimated theoretically. It is only necessary to take a momentum balance across planes cutting the tunnel test section far upstream and far downstream, as shown in Figure 11. The propeller thrust is given by:

$$T = \rho A_1 U_1 (U_2 - U_o) + \rho A_{2_o} U_c (U_c - U_o) + A_o (p_c - p_o) \qquad [54]$$

Continuity considerations require that

$$A_o U_o = A_1 U_1 + A_{2_o} U_c \qquad [55]$$

Using these, and non-dimensionalizing, the following results:

$$C_T = \frac{U_1}{U_o}\left[2\left(\frac{U_2}{U_o} - \frac{U_c}{U_c}\right)\right] + \frac{A_o}{A_1}\left[2\,\frac{U_c}{U_o} - (2+\sigma_o)\right] \qquad [56]$$

The velocities U_1 and U_2 have earlier been related to the propeller characteristics through Equations [13] and [12] and U_c/U_o has been defined as $\sqrt{1+\sigma_o}$. Using these relationships, Equation [56] becomes:

$$C_T = 2\left[\sqrt{1+\sigma_o+C_T/\eta_c} - \sqrt{C_T(1-\eta_c)/\eta_c}\right]\left[\sqrt{1+\sigma_o+C_T/\eta_c} - \sqrt{1+\sigma_o}\right]$$

$$+ \frac{A_o}{A_1}\left[2\sqrt{1+\sigma_o} - (\sigma_o + 2)\right] \qquad [57]$$

This relationship only applies when the flow is choked, so that from it, the conditions of propeller operation at which choking occurs may be related to the ratio of tunnel to disc area:

$$\frac{A_o^*}{A_1} = \frac{\left[\sqrt{1+\sigma_o+C_T/\eta_c} - \sqrt{1+\sigma_o}\right]\left[\sqrt{1+\sigma_o+C_T/\eta_c} - \sqrt{C_T(1-\eta_c)/\eta_c}\right] - C_T/2}{\left[\frac{(\sigma_c+2)}{2} - \sqrt{1+\sigma_o}\right]} \qquad [58]$$

For small values of C_T/η_c and σ_o this becomes:

$$\frac{A_o^*}{A_1} \sim \frac{4C_T}{\sigma_o^2}\left(\frac{1-\eta_c}{\eta_c}\right) \qquad [59]$$

In the case of a stationary drag disc ($\eta_c = -\infty$; $C_T = -C_D$), Equation [59] reduces to precisely the result which may be obtained directly from momentum considerations:

$$\frac{A_o^*}{A_1} \sim \frac{4C_D}{\sigma_o^2} \qquad [60]$$

Charts based on Equation [58] from which choking conditions may be estimated are presented as Figures 12a - 12e . Theoretical critical tunnel area ratios corresponding to the data presented in Figure 10 are also tabulated below.

TABLE 1

Theoretical Tunnel Area Ratios Corresponding to Choking

A_o^*/A_1(theor)	3.13	3.69	4.37	4.96
σ_o	1.3	.7	.32	.25
A_o^*/A_1(actual) = 4.70 in all cases.				

One more comment might be made about measurements of supercavitating propeller characteristics. For subcavitating propellers the actuator disc picture of the flow leads to the prediction that the axial flow velocity in the plane of the disc but outside of it is identical with the velocity of the free stream. For this reason the speed in the propeller plane is sometimes measured and used in place of a speed measurement in the flow far ahead of the screw. It should be clear from the picture of the flow presented here that the speed of the flow in the plane of a supercavitating propeller is <u>not</u> even approximately equal to the free stream speed in the general case. The effective approach speed must therefore be measured sufficiently far ahead of the screw. In making such measurements adequate recognition must be given to the effect upon the pressures at the tunnel walls which may be caused by an obstacle like a heavily supercavitating propeller.

SUMMARY AND CONCLUSIONS

Based entirely on momentum and other simple considerations a reasonably complete picture of the one-dimensional pressure and velocity fields associated with heavily supercavitating propellers and drag discs has been constructed. The results are summarized in Figures 3 - 8 .

It is crucial in developing a useful momentum theory for these flows to take into account the blade cavitational efficiency (η_c) associated with the disc, since this quantity must be influential in determining the extent and volume of the cavities shed by the blades. The opportunity to introduce this quantity arises naturally since the head increase which occurs across the disc may be shown to equal the ratio of thrust coefficient (C_T) and η_c. It may also be shown, although this is not done here, that this latter relation for the head increase across the disc adequately takes into account the effect of the flow rotation behind the disc.

A momentum balance for the flow within the momentum control surface shown in Figure 4 yields a relationship between the inflow speed and C_T, η_c, and σ_c (free stream cavitation number). It is shown that the flow is very often <u>retarded</u> while approaching a heavily supercavitating propeller, so that the so-called ideal efficiency, η_i, of such a propeller takes on values in excess of unity. The ideal efficiency actually increases with decreasing blade cavitational efficiency; however, the net efficiency ($\eta_i \cdot \eta_c$) at the same time decreases. This retardation causes a reduction of thrust deduction, or even a change in its sign References 8, 18, and 19.

At zero free stream cavitation number ($\sigma_o = 0$) the inflow must always be retarded.

For positive values of σ_o accelerated inflow speeds occur but are restricted in value by the necessity to maintain pressures in the inflow higher than cavity pressure. Conditions corresponding to the limiting inflow speed are estimated. It is shown that an absolute maximum net efficiency exists corresponding to operation at this limiting condition. It is noted that these maximum efficiencies imply larger values of η_c than have been realized in practice, so that they have not so far been approached.

Charts are provided in this report from which the inflow speed may readily be estimated for use in predicting the performance of heavily supercavitating propellers.

In an unbounded stream the cavity length is finite for $\sigma_o > 0$ and is infinite for $\sigma_o = 0$. The cavity maximum diameter is shown in the latter case to be finite only when the inflow and free stream speeds are identical.

In the case of cavities of finite length, a loss of head occurs across the region of cavity collapse (plane 3 in Figure 4) and formulae for the head in the wake are given. This is higher than the free stream head for a thrusting propeller and lower for a drag disc. The outflow speed just behind the region of cavity collapse is shown to be greater than the inflow speed for all cases of retarded inflow and for moderate degrees of accelerated inflow; for sufficiently large thrusts the reverse may be true. Formulae are given for these outflow speeds.

The effects of tunnel boundaries are discussed. It is shown that no corrections to inflow speed are required for a supercavitating propeller operating either in an open jet or between solid walls; this is somewhat in contrast to the case of the subcavitating propeller for which inflow speeds must be corrected for the presence of solid walls. The phenomena of tunnel choking is discussed and momentum considerations are applied to the calculation of conditions for which infinite cavity length occurs at positive non-zero ($\sigma_o > 0$) cavitation numbers during operation between solid walls. A comparison between measured and predicted values of the critical ratio of tunnel area to screw area is presented.

The results presented herein make it quite clear that the distribution of flow velocities and pressures which attend the operation of a heavily supercavitating propeller will not at all correspond to the predictions of theory for subcavitating propellers. The use of the latter predictions is thus unjustified. Even for a relatively weakly supercavitating propeller it seems problematical that predictions of inflow speed based on subcavitating propeller theory are useful.

The present theory has assumed a propeller with an infinite number of blades and one-dimensional flow. These assumptions are briefly discussed herein. The conditions under which the predictions of this theory reasonably apply are not clear, but when the propeller blade elements operate at loadings such that blade interference or cascade effects dominate the flow through the blade, then it seems likely that the present theory provides a

reasonable approximation to the general features of the real flow.

It would clearly be very useful to obtain some quantitative experimental evidence relating to the details of the flow field about supercavitating propellers or drag discs, such as are predicted by the present theory. It would be particularly useful to obtain measurements of the inflow speed as a function of C_T, η_c, and σ_o.

There remain many interesting questions concerning flows past supercavitating propellers and drag discs which are left for more elaborate theory to discuss. These include: What is the relationship between the length of the cavity and C_T, η_c, and σ_o?; what shape does the cavity boundary take?; what is the general asymptotic shape of the cavity for $\sigma_o = 0$?; does the flow speed on the axis of symmetry change monotonically from far upstream to the disc?; how are the predictions made here modified by a finite number of blades?; and, what is the optimum distribution of spanwise loading for a supercavitating propeller?

REFERENCES

1. Posdunine, V L., "On the Working of Supercavitating Screw Propellers," (in English!), Doklady AN SSSR, Vol. XXXIX, No. 8, 1943; Also, Transactions of the Institute of Naval Architects, Vol. 86, 1944.

2. Posdunine, V. L., "The Construction and Performance of Supercavitating Propellers," Izv. OTN AN SSSR, Nos. 1-2, 1945.

3. Posdunine, V. L., "Basic Theory of the Construction and Performance of Supercavitating Propellers," Izv. OTN AN SSSR, Nos. 10-11, 1945.

4. Tulin, M. P., and Burkart, M. P., "Linearized Theory for Flows About Lifting Foils at Zero Cavitation Number," DTMB Report C-638, February 1955.

5. Tachmindji, A. J., Morgan, W. B., Miller, M. L., and Hecker, R., "The Design and Performance of Supercavitating Propellers," DTMB Report C-807, February 1957.

6. Tachmindji, A. J., and Morgan, W. B., "The Design and Estimated Performance of a Series of Supercavitating Propellers," Proceedings of the 2nd ONR Symposium on Naval Hydrodynamics, (Government Printing Office) Washington, D. C., 1958.

7. Venning, E., and Haberman, W. L., "Supercavitating Propeller Performance," Transactions of the SNAME, Vol. 70, 1962.

8. Tulin, M. P., "Supercavitating Propeller — History, Operating Characteristics, Mechanism of Operation," Proceedings of the 4th (1962) ONR Symposium on Naval Hydrodynamics, (Government Printing Office) Washington, D. C., 1964.

9. Johnson, C. - A., "Comparison of Propeller Design Techniques," Proceedings 4th (1962) ONR Symposium on Naval Hydrodynamics, (Government Printing Office) Washington, D. C., 1964.

10. Basin, A. M., "On the Theory of the Ideal Cavitating Propeller," Doklady AN SSSR, Vol. 49, 1945.

11. Lavrent'yev, V. M., "Theory of the Ideal Cavitating Propeller," Doklady AN SSSR, Vol. 50, 1945.

12. Epshteyn, L. A., "On the Action of the Ideal Supercavitating Propeller," Inzhenerniy Sbornik, Vol. 9, 1951.

13. Küchemann, D., and Weber, J., "Aerodynamics of Propulsion," McGraw-Hill, New York, 1953.

14. Yim, B., "The Flow Field of an Infinitely Bladed Propeller with Radially Non-Uniform Loading," HYDRONAUTICS, Incorporated Technical Report 005-2, February 1961.

15. Glauert, H., "Airplane Propellers," Vol. IV, Aerodynamic Theory, (N. Durand, ed.) Durand Reprinting Committee, Pasadena, California, 1943.

16. Tulin, M. P., "Supercavitating Flows," in Handbook of Fluid Dynamics, V. Streeter, ed., McGraw Hill, 1961.

17. van de Voorde, C. B., and Esveldt, J., "Tunnel Tests on Supercavitating Propellers," Proceedings of the Fourth (1962) ONR Symposium on Naval Hydrodynamics, (Government Printing Office), Washington, D. C., 1964.

18. Bavin, V. F., and Miniovich, I. J., "Experimental Investigations of Interaction Between Hull and Cavitating Propeller," Contribution of the Leningrad Ship Model Basin, USSR, to the 10th International Towing Tank Conference, London, September 1963.

19. Beveridge, J. L., "Induced Velocity Field of a Fully Cavitating Propeller on Interaction Experiments with Fully Cavitating Propeller Behind a Hydrofoil," DTMB Report 1832, April 1964.

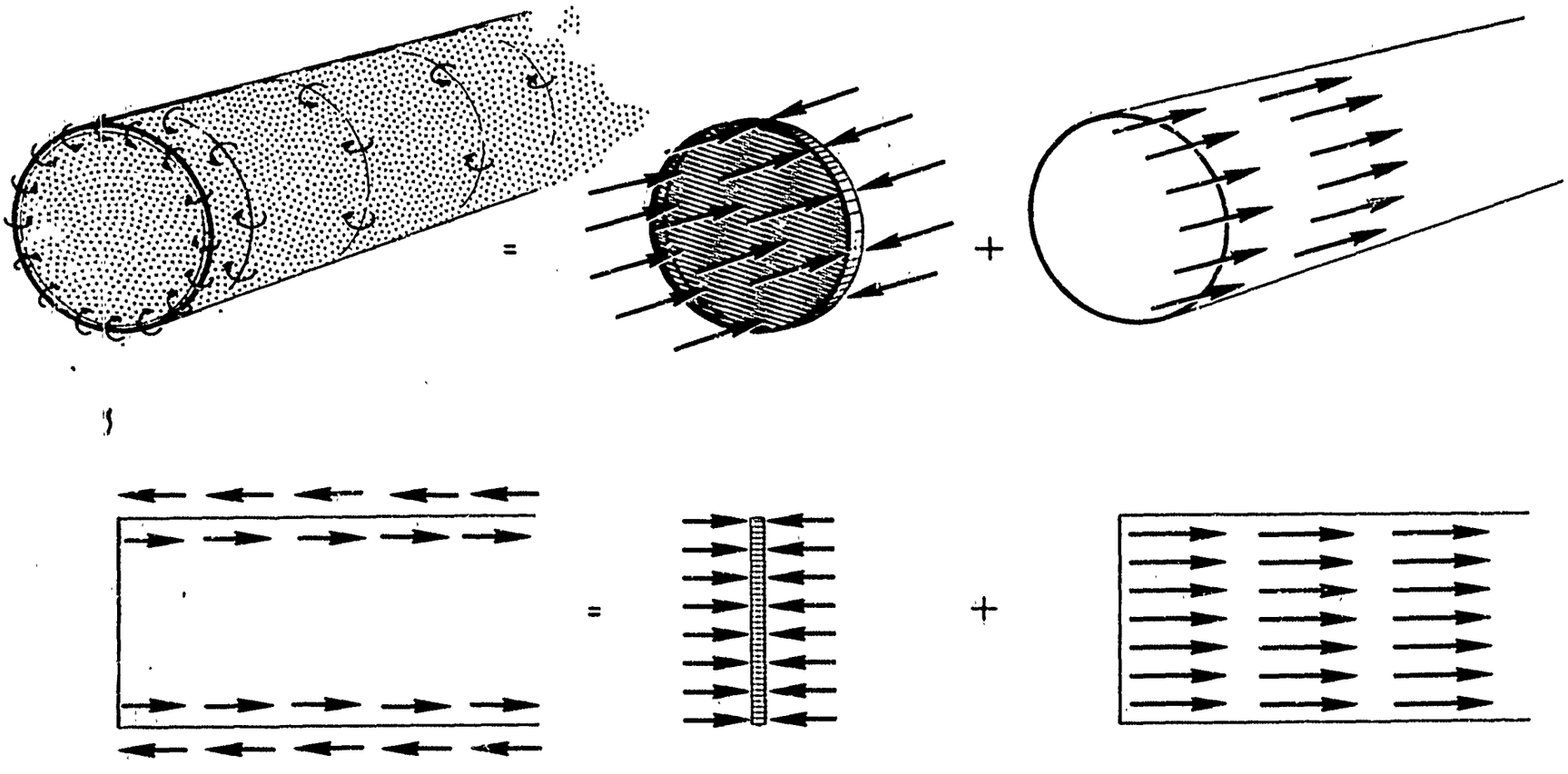

FIGURE 1– EQUIVALENCE BETWEEN VORTEX SHEATH AND SINK DISC FLOWS

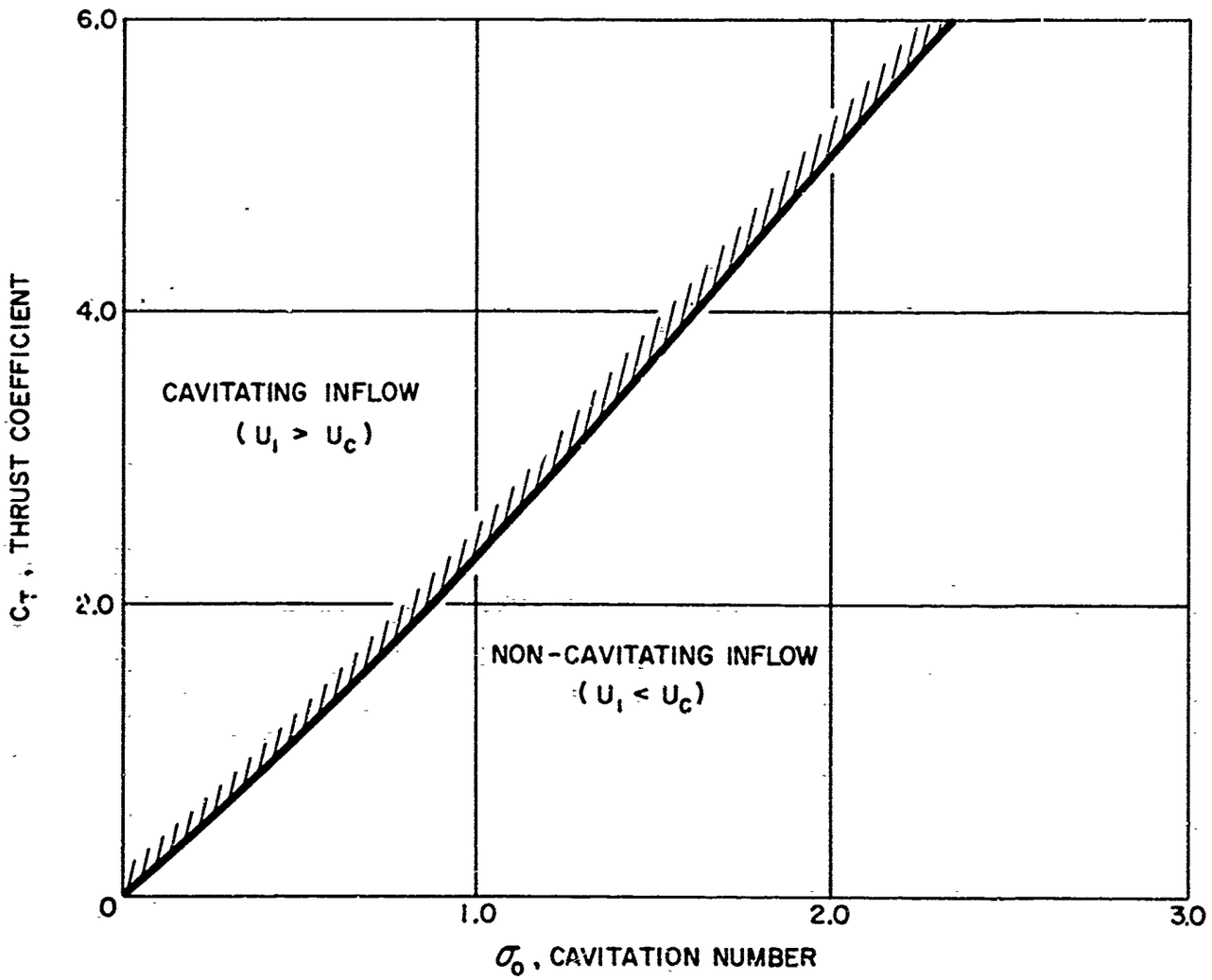

FIGURE 2 – SUBCAVITATING MOMENTUM THEORY – INFLOW CAVITATION

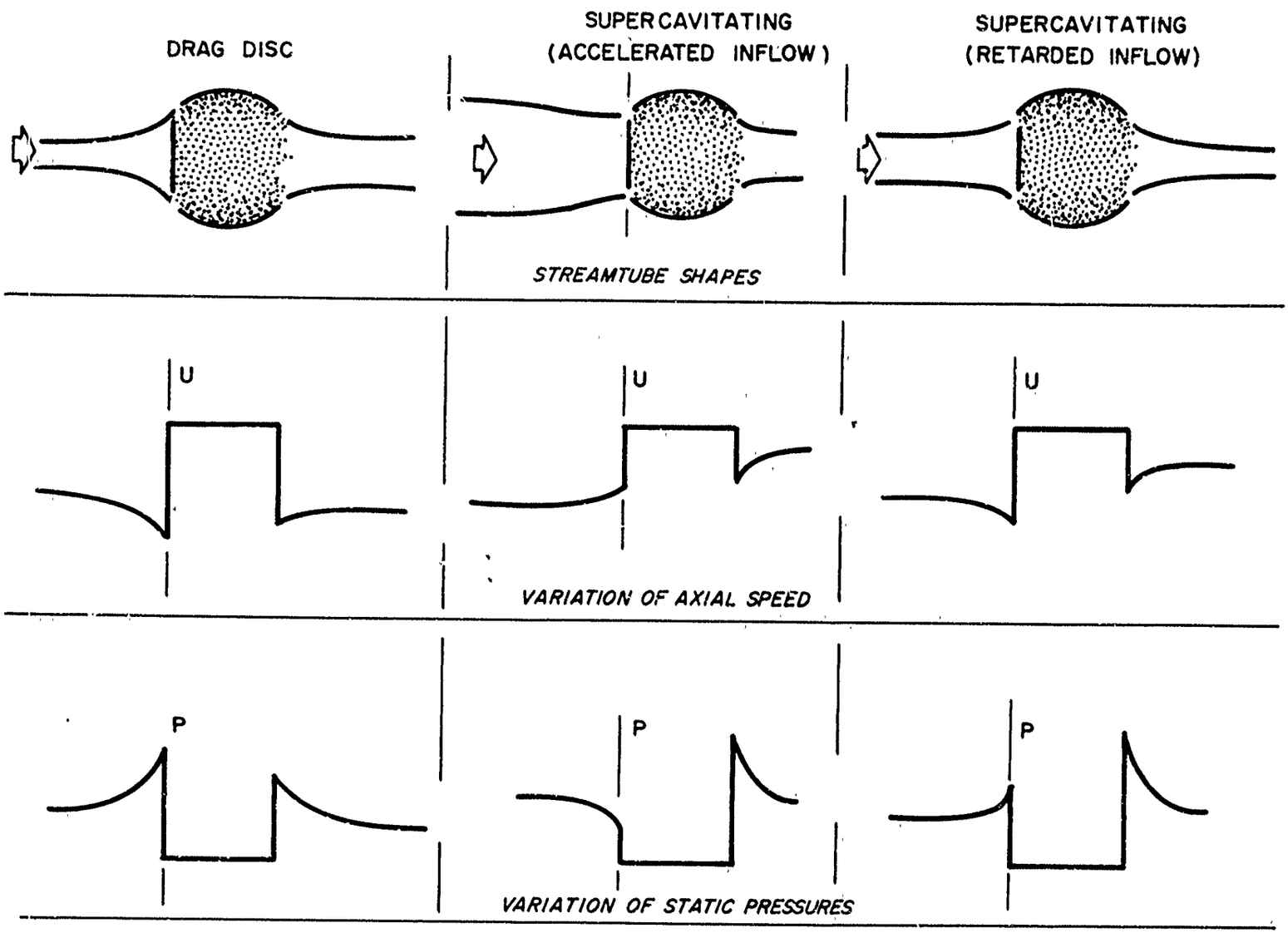

FIGURE 3- SCHEMATIC FLOWS PAST A DRAG DISC AND SUPERCAVITATING PROPELLERS

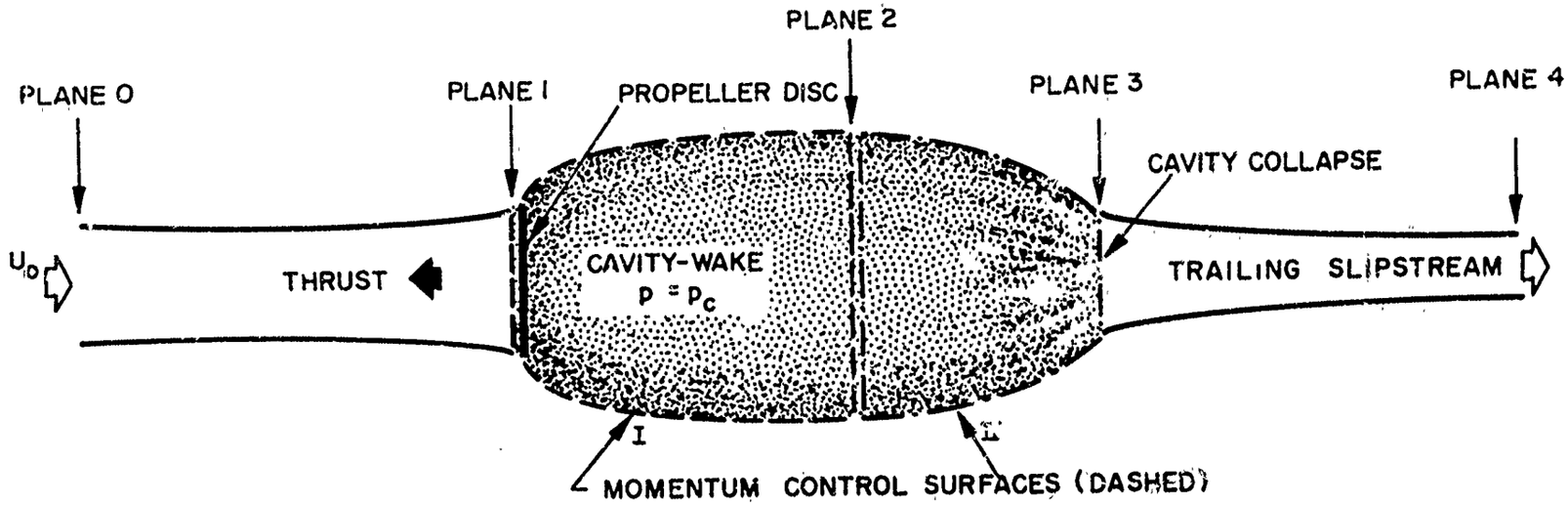

FIGURE 4– SCHEMATIC OF FLOW AND CONTROL SURFACES

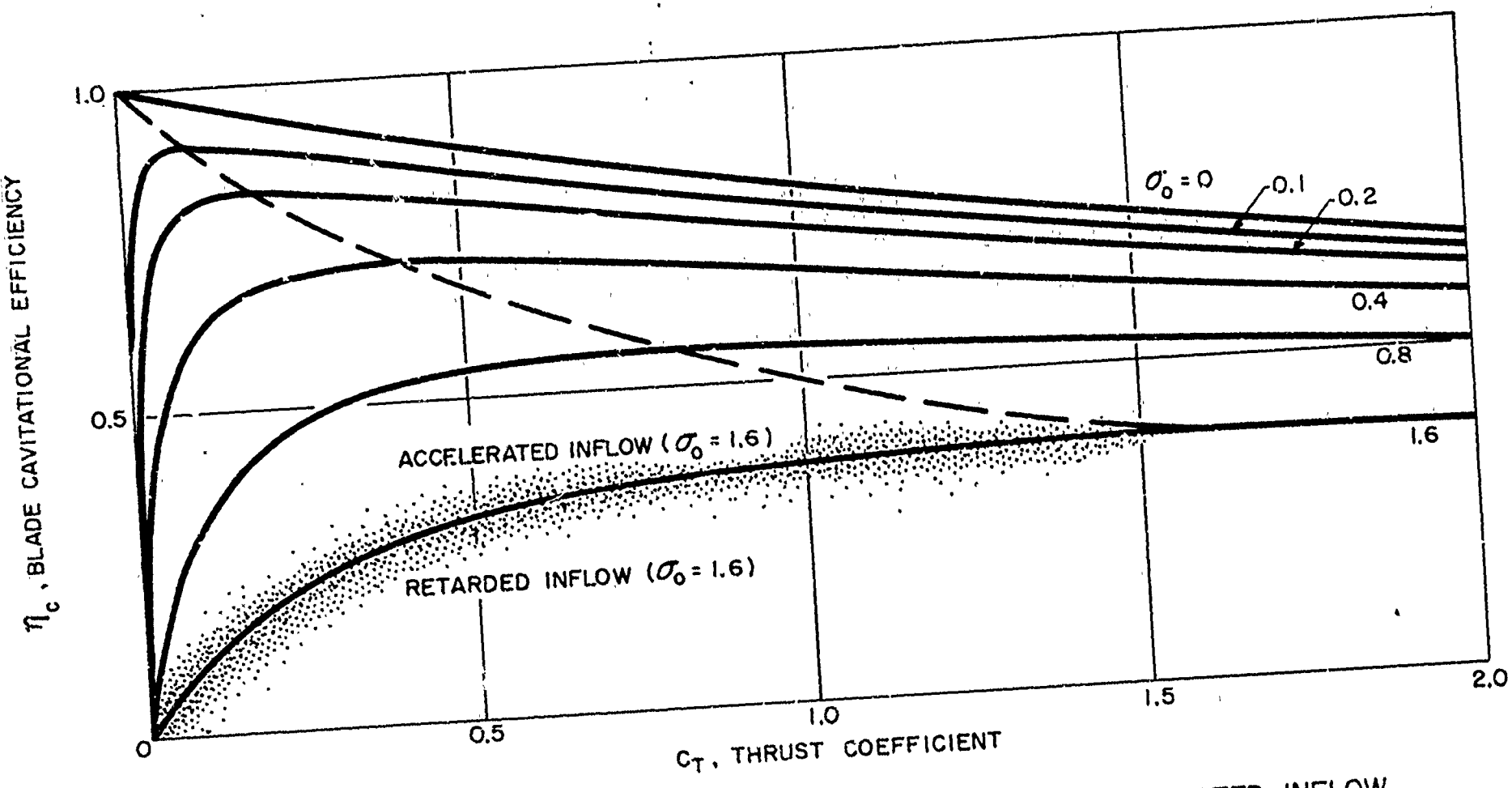

FIGURE 5— BOUNDARIES BETWEEN RETARDED AND ACCELERATED INFLOW FOR SUPERCAVITATING PROPELLERS

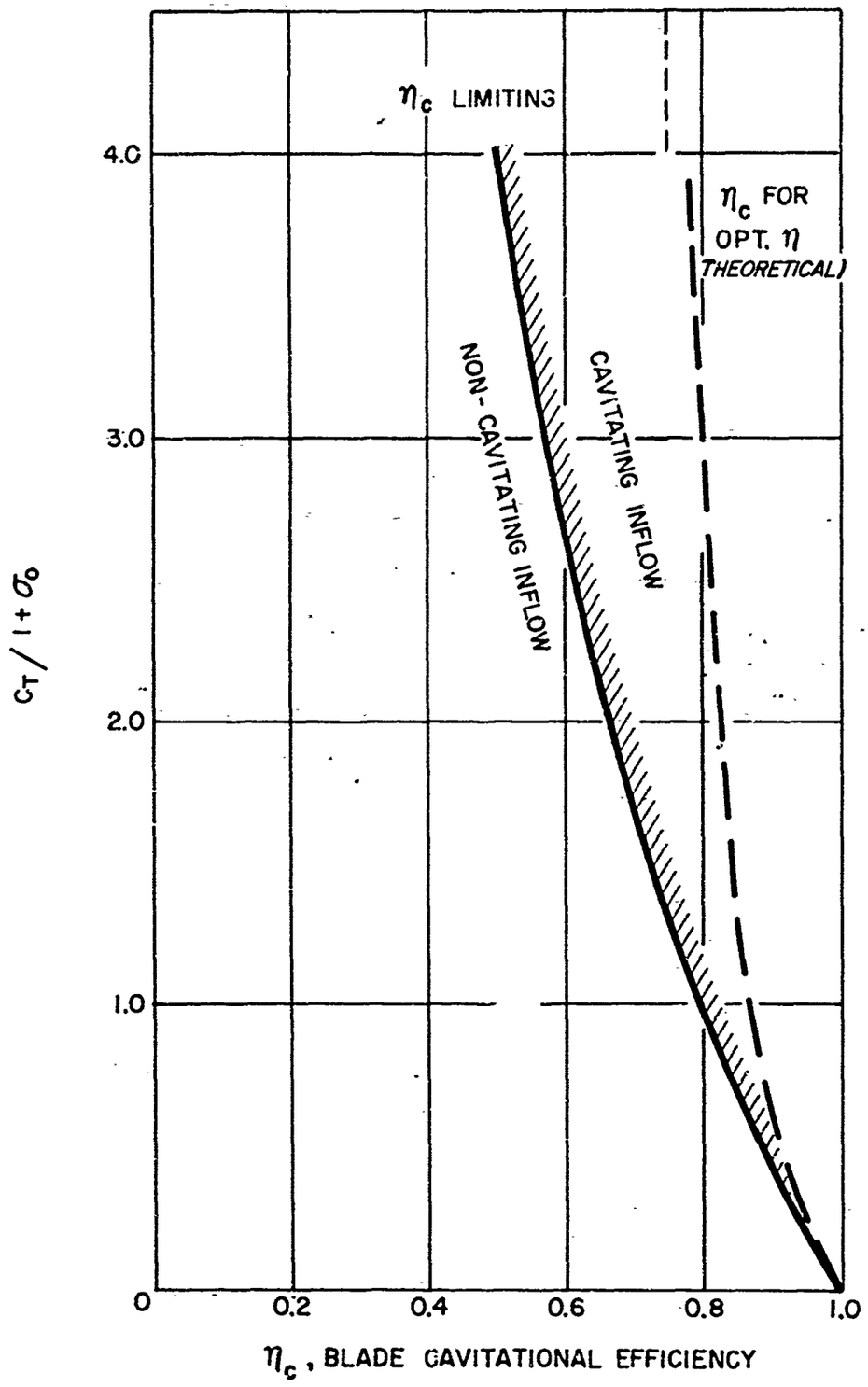

FIGURE 6— LIMITING η_c VERSUS $C_T/1+\sigma_0$

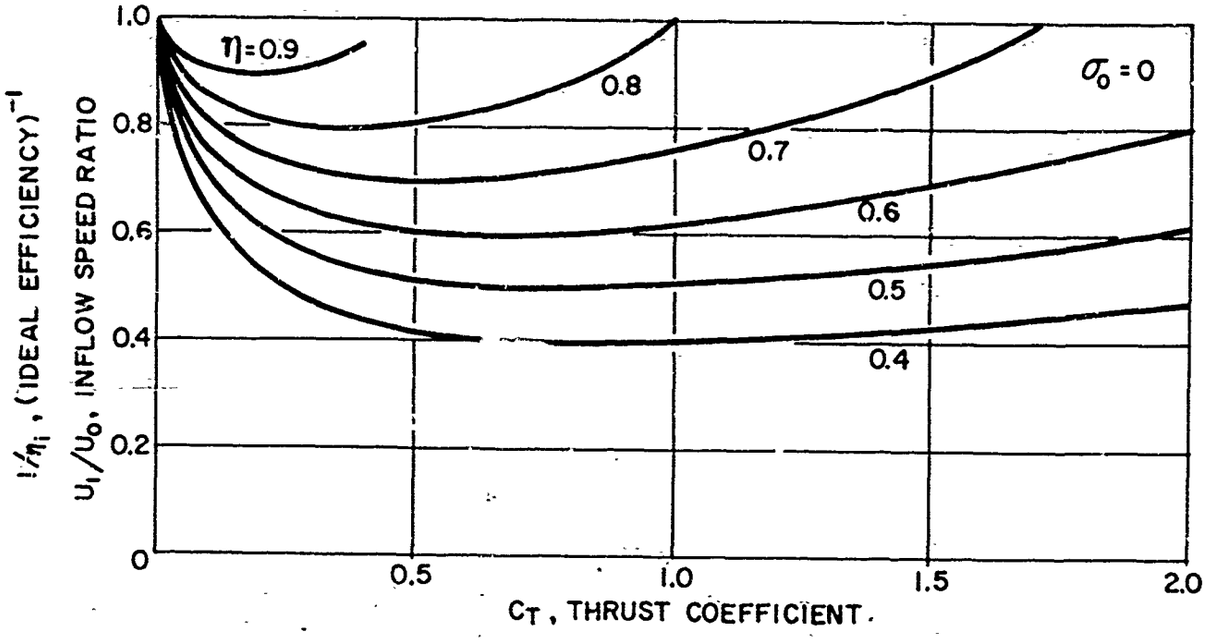

FIGURE 7a— INFLOW SPEED,(IDEAL EFFICIENCY)$^{-1}$ VERSUS THRUST COEFFICIENT; $\sigma_0 = 0$

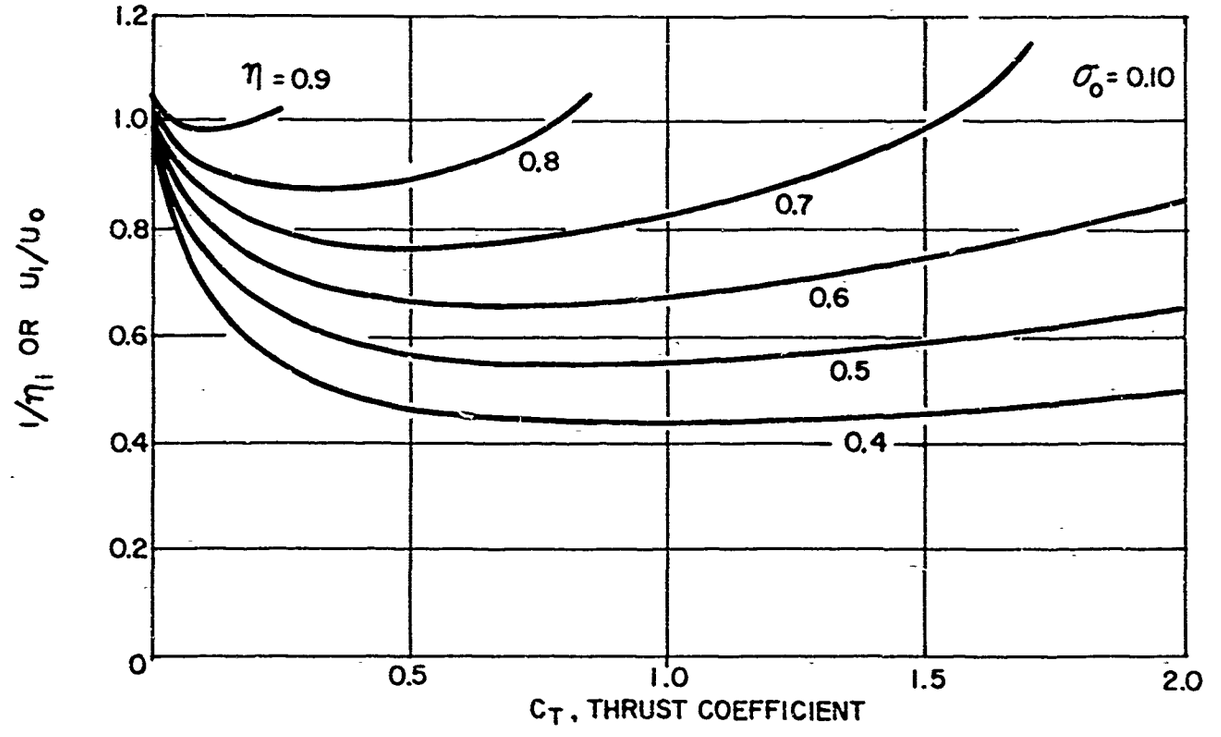

FIGURE 7b— U_I/U_o VERSUS C_T; $\sigma_0 = 0.10$

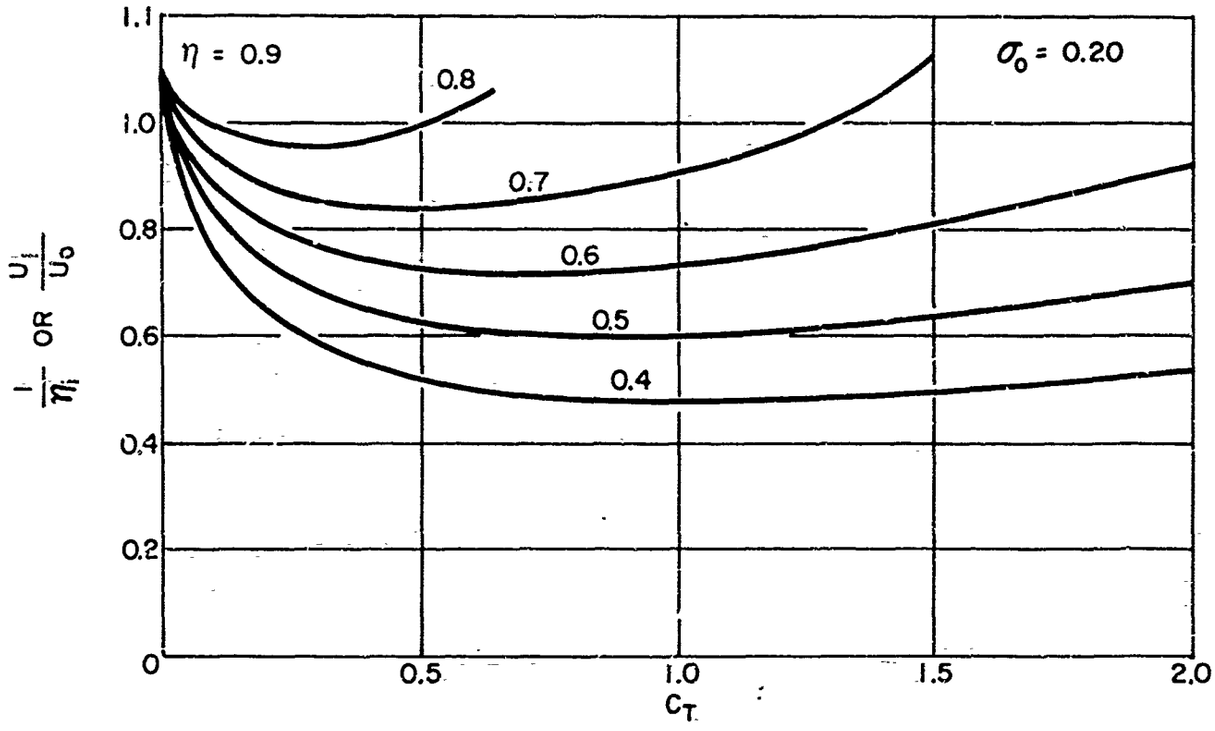

FIGURE 7c— U_1/U_0 VERSUS C_T ; σ_0 = 0.20

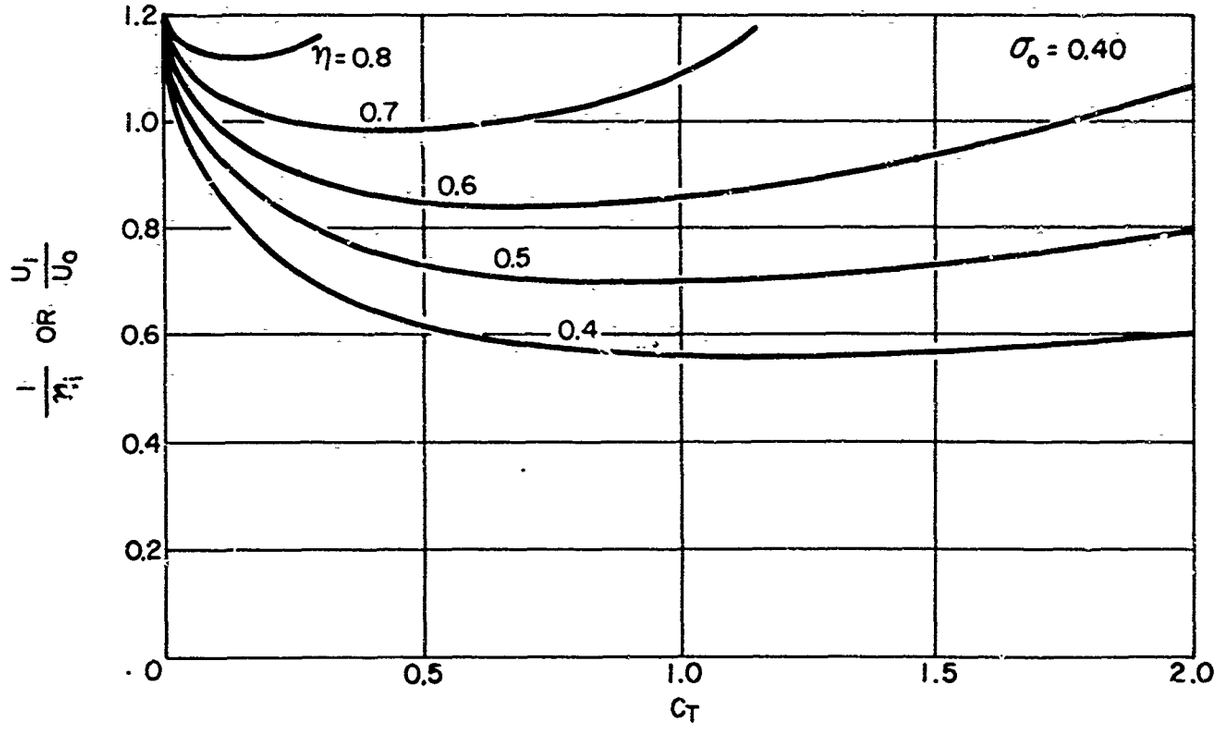

FIGURE 7d— U_1/U_0 VERSUS C_T ; σ_0 = 0.40

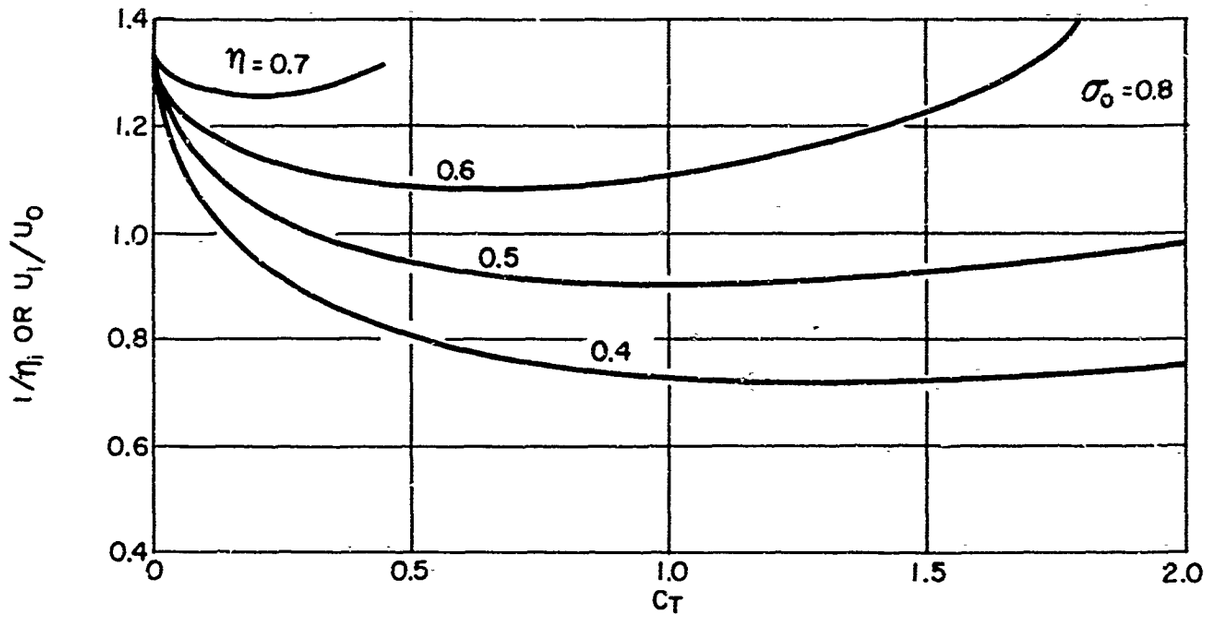

FIGURE 7e– U_1/U_0 VERSUS C_T ; $\sigma_0 = 0.80$

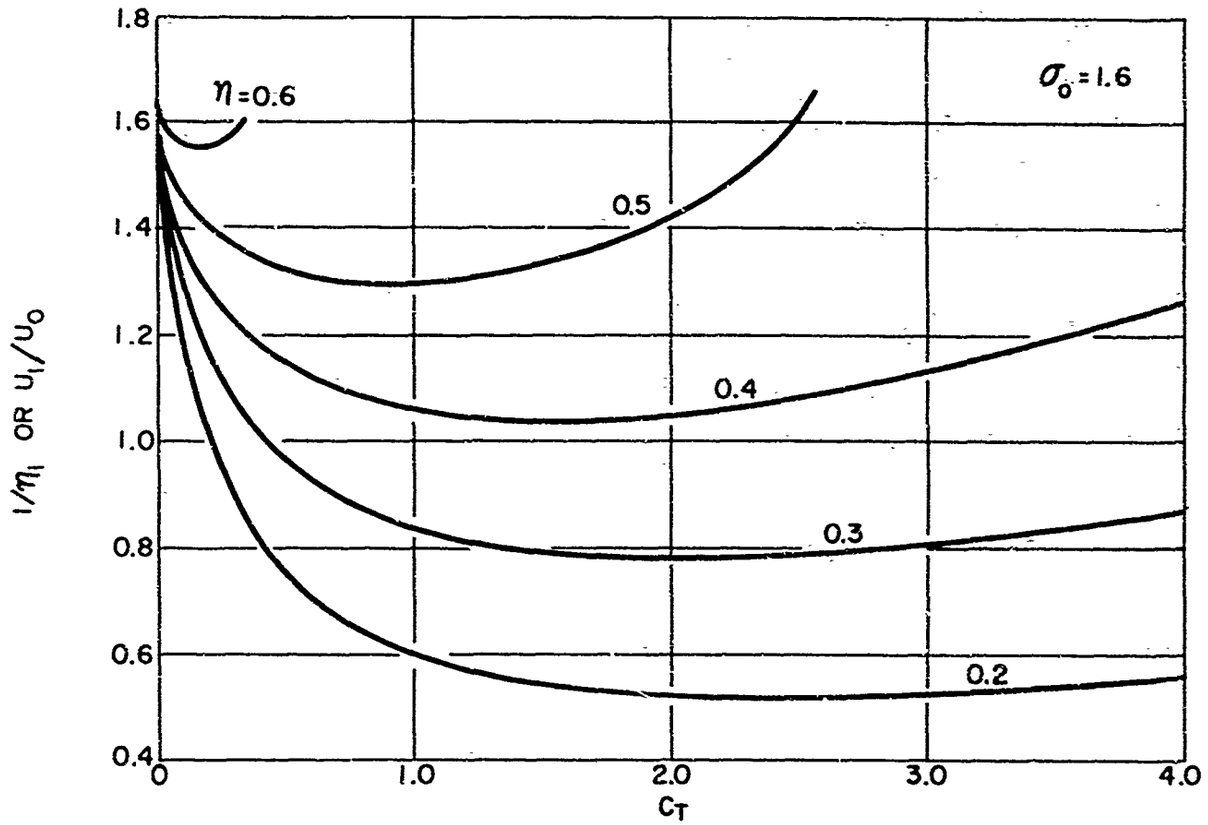

FIGURE 7f– U_1/U_0 VERSUS C_T ; $\sigma_0 = 1.6$

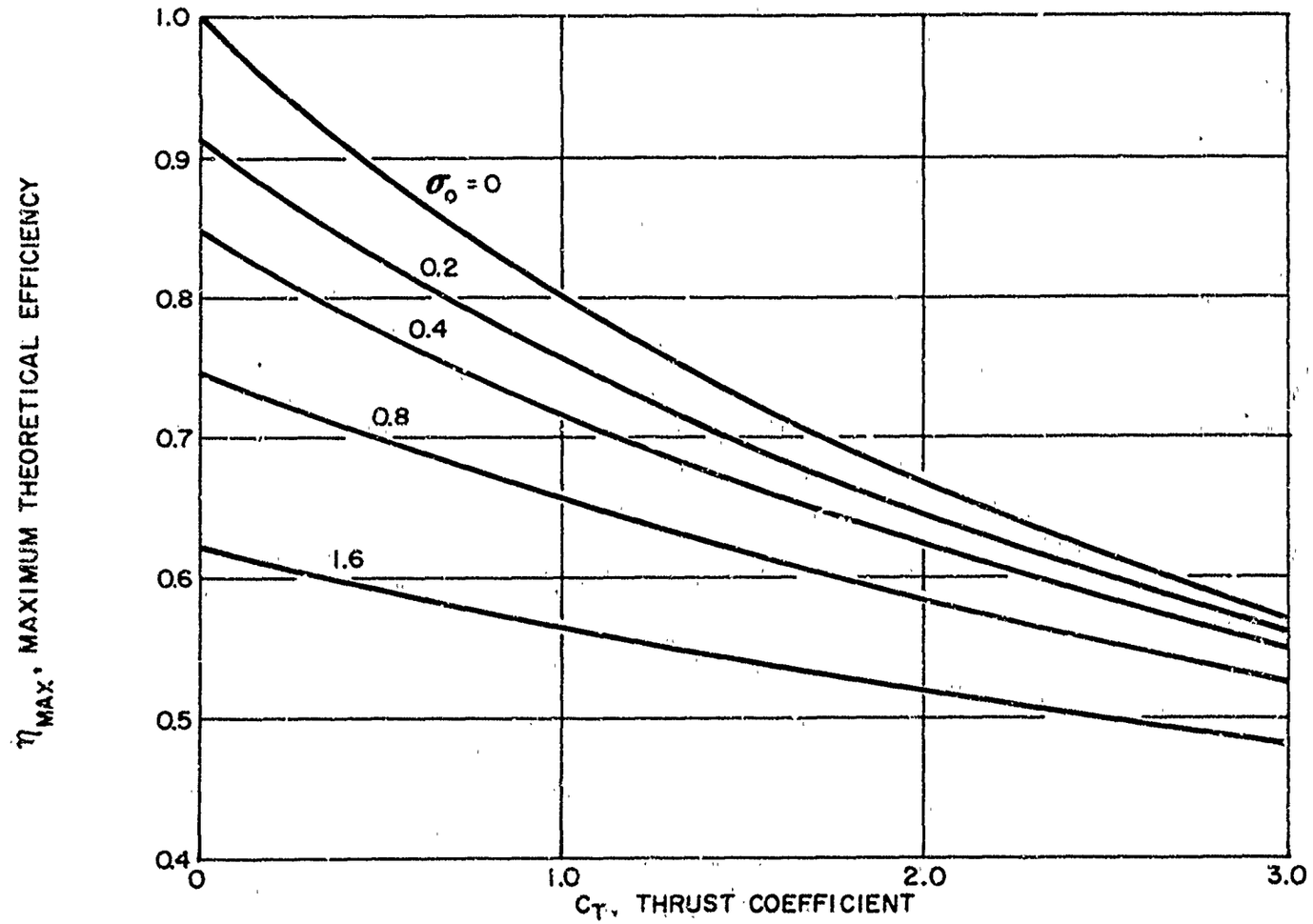

FIGURE 8— MAXIMUM EFFICIENCY (THEORY) VERSUS C_T FOR SUPERCAVITATING PROPELLERS

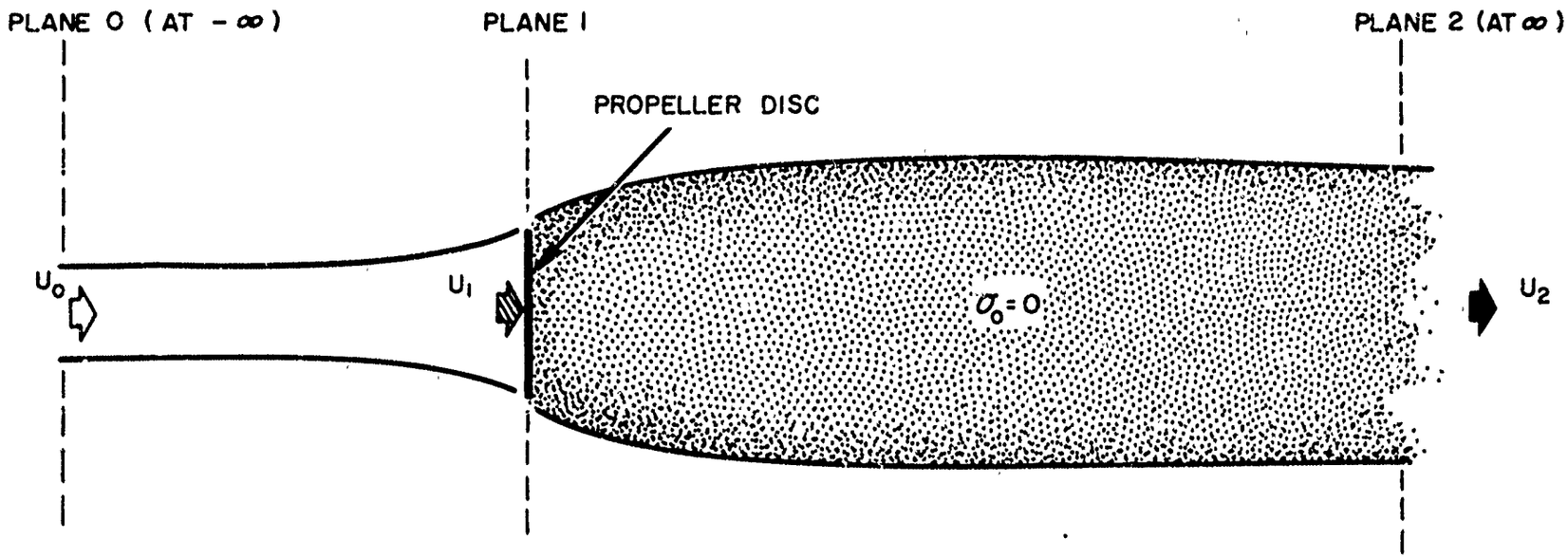

FIGURE 9— SCHEMATIC OF ASSUMED SUPERCAVITATING PROPELLER FLOW, $\sigma_0 = 0$

(THE ASSUMPTION THAT THE CAVITY DIAMETER IS BOUNDED AT ∞ IS SHOWN IN THE TEXT TO BE INCORRECT , UNLESS $U_1 \equiv U_0$)

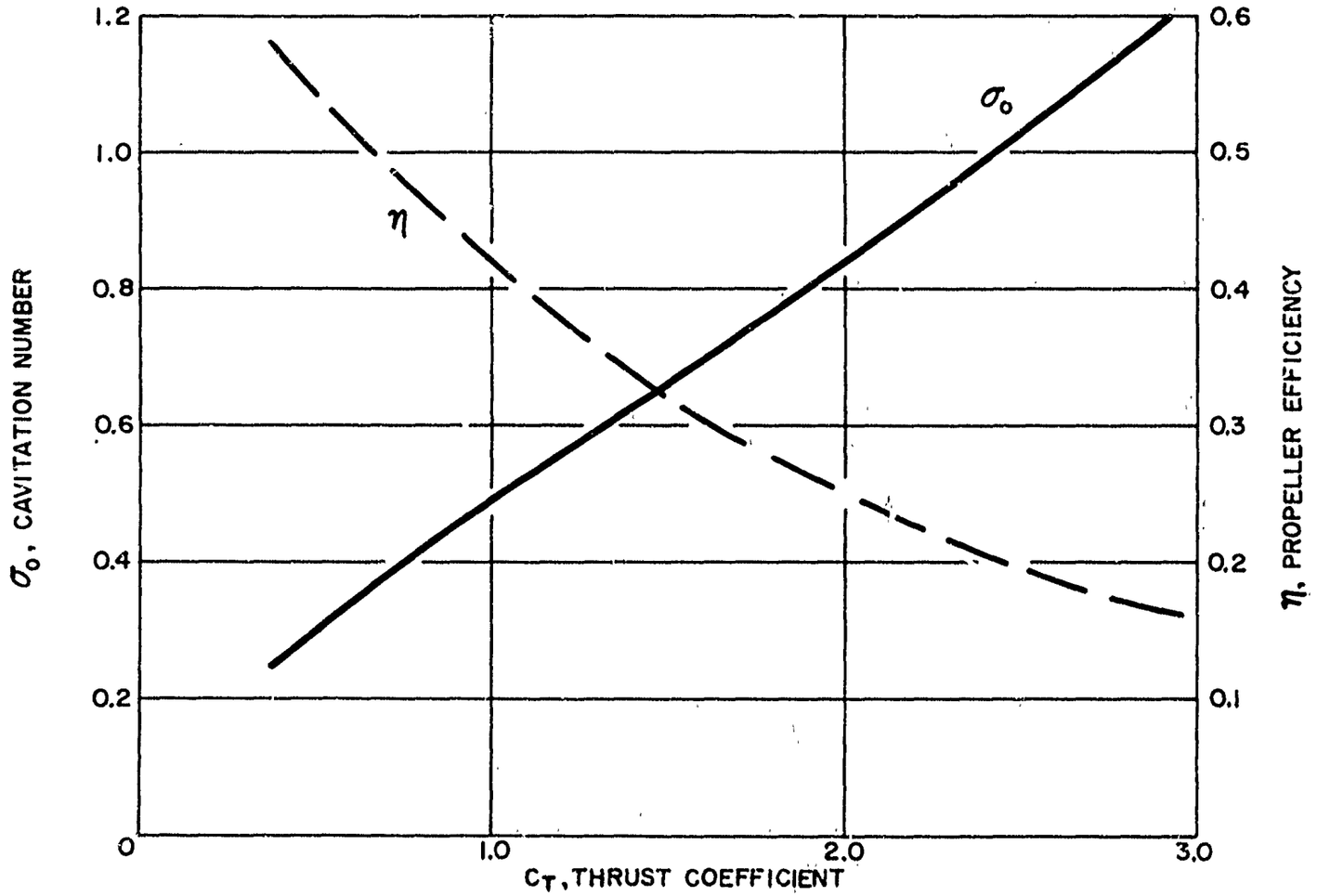

FIGURE 10— CHOKING OPERATING CONDITIONS (EXP'T.) FOR HYDRONAUTICS SUPERCAVITATING PROPELLER H3—A IN SOLID-WALL TUNNEL. PROP. DIAM. = 0.2602 m.; TUNNEL CROSS-SECTION = 0.25 m^2

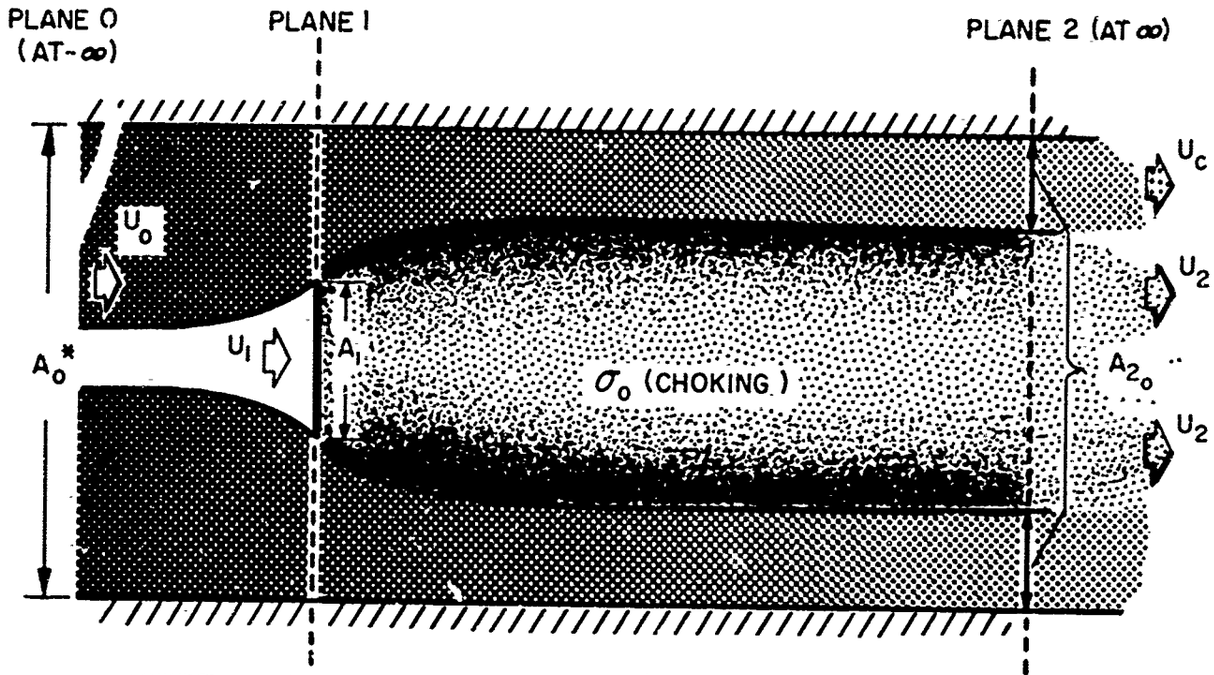

FIGURE II– SCHEMATIC OF A SUPERCAVITATING PROPELLER FLOW CHOKING A SOLID-WALLED WATER TUNNEL

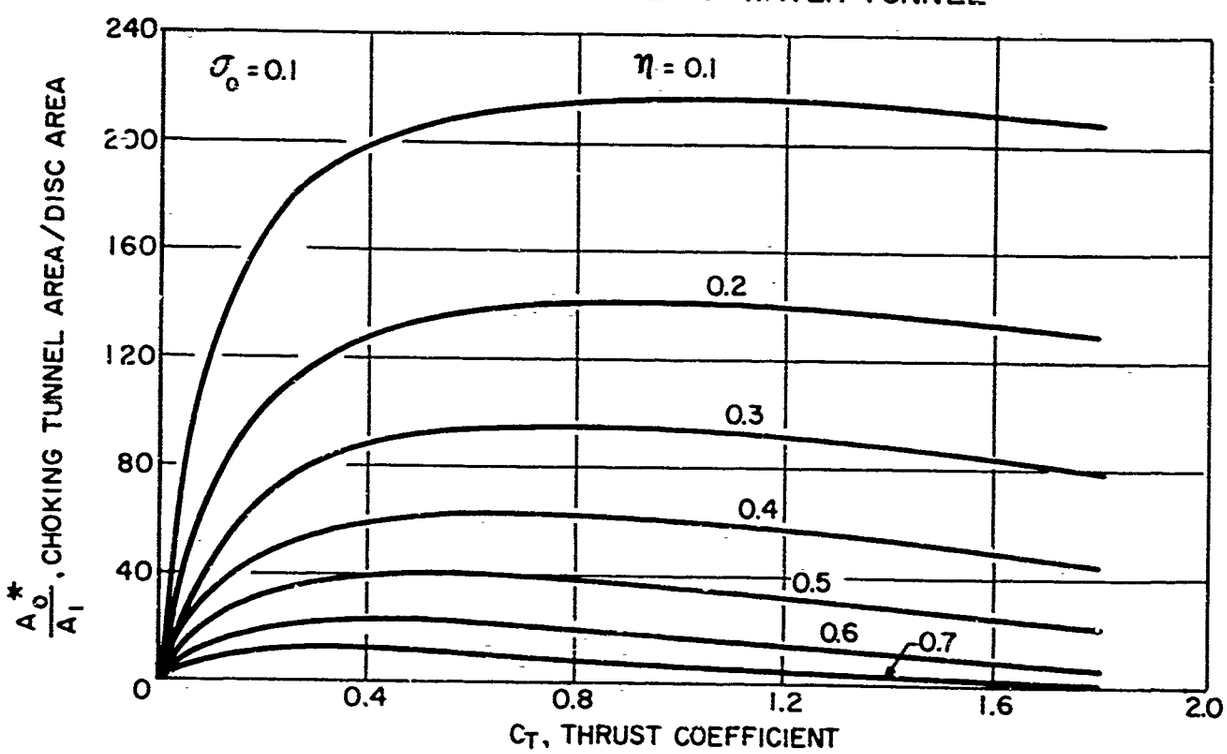

FIGURE 12a– CHOKING AREA RATIOS VERSUS THRUST COEFFICIENT, $\sigma_0 = 0.1$

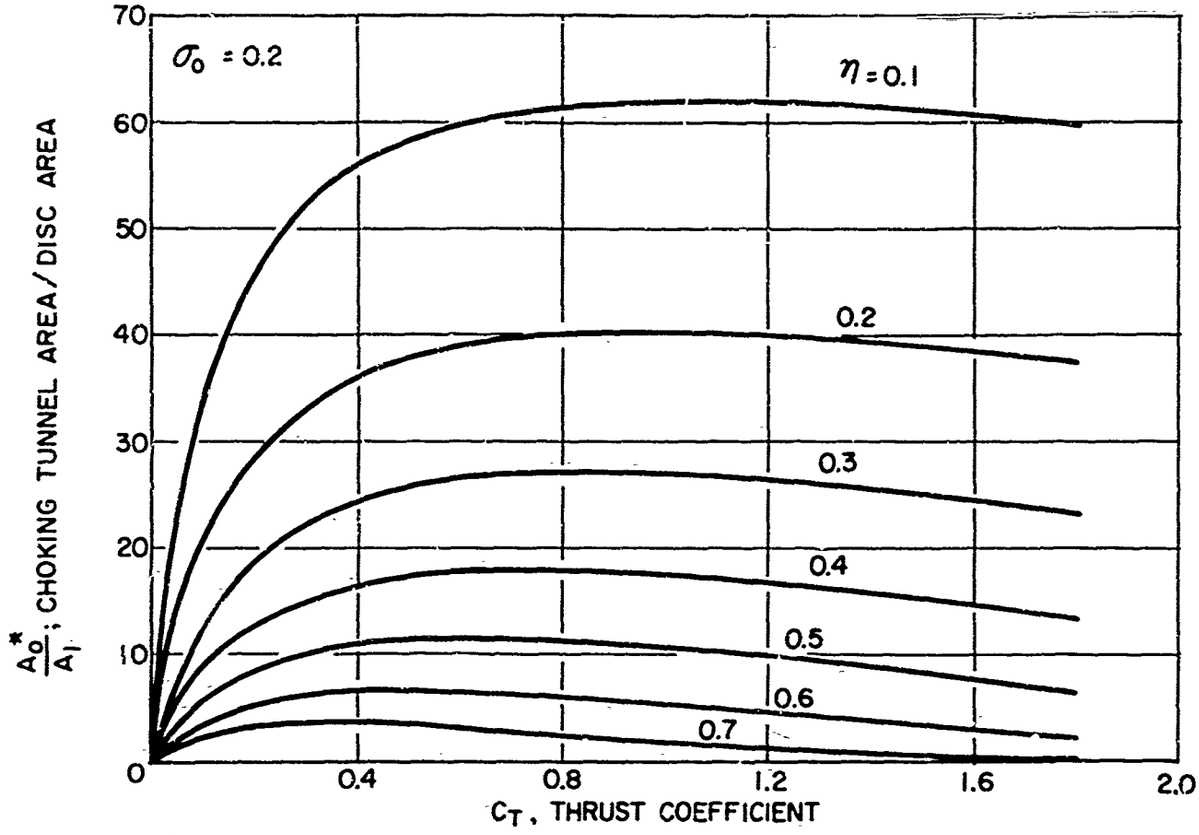

FIGURE 12b— A_0^*/A_1 VERSUS C_T, $\sigma_0 = 0.2$

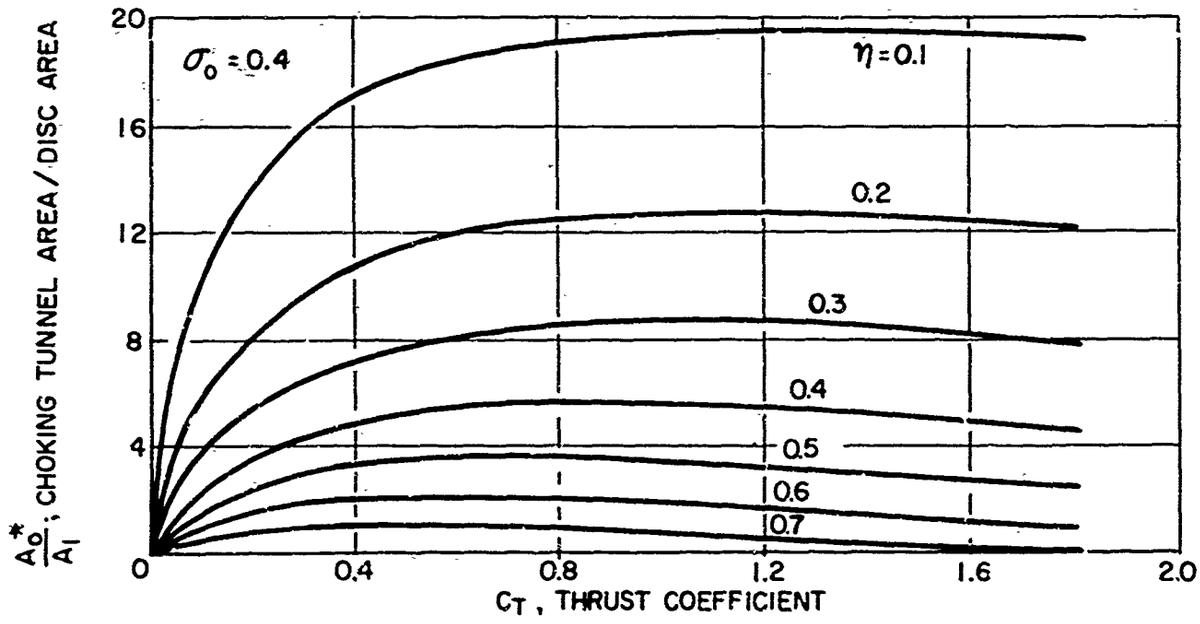

FIGURE 12c— A_0^*/A_1 VERSUS C_T, $\sigma_0 = 0.4$

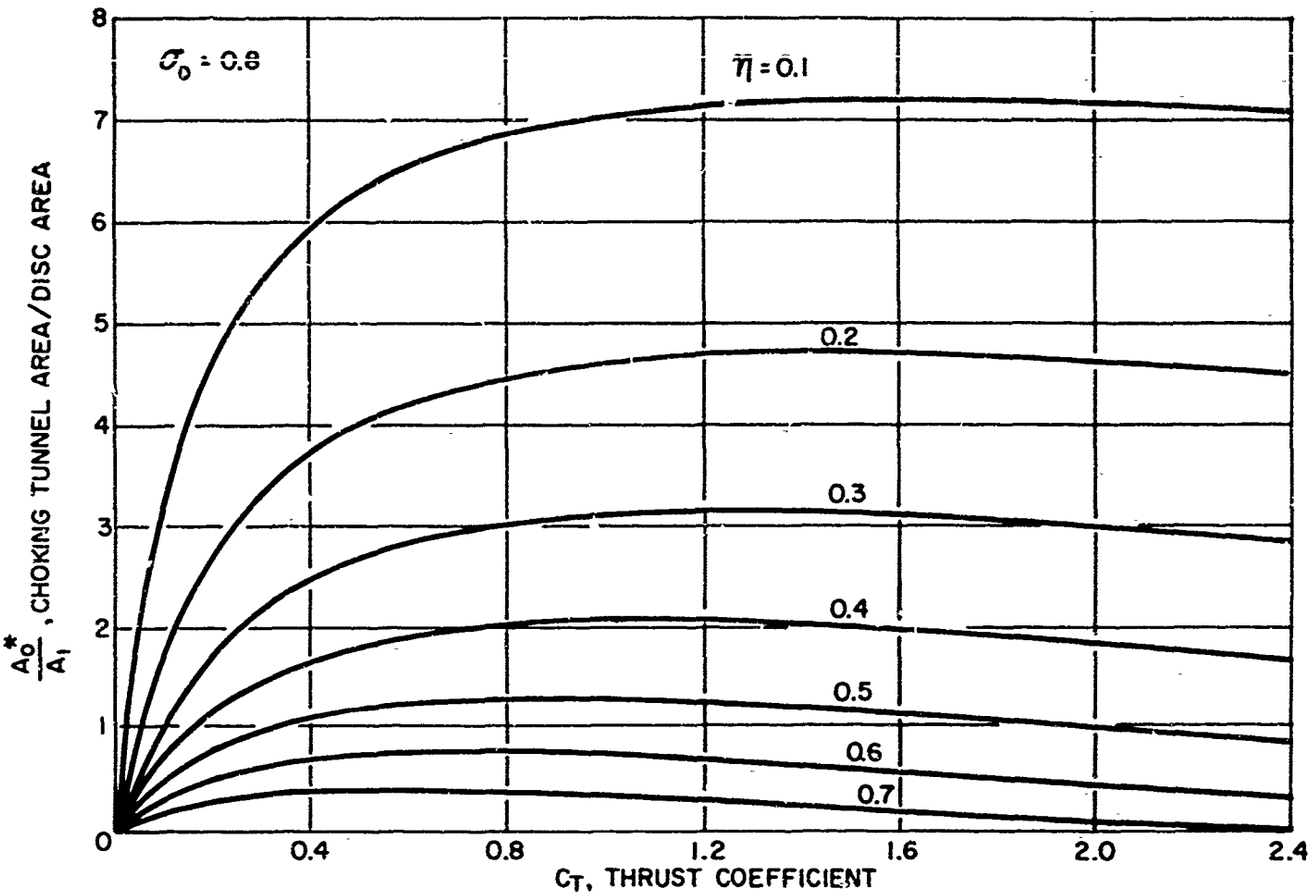

FIGURE 12d– A_0^*/A_1 VERSUS C_T , σ_0 = 0.8

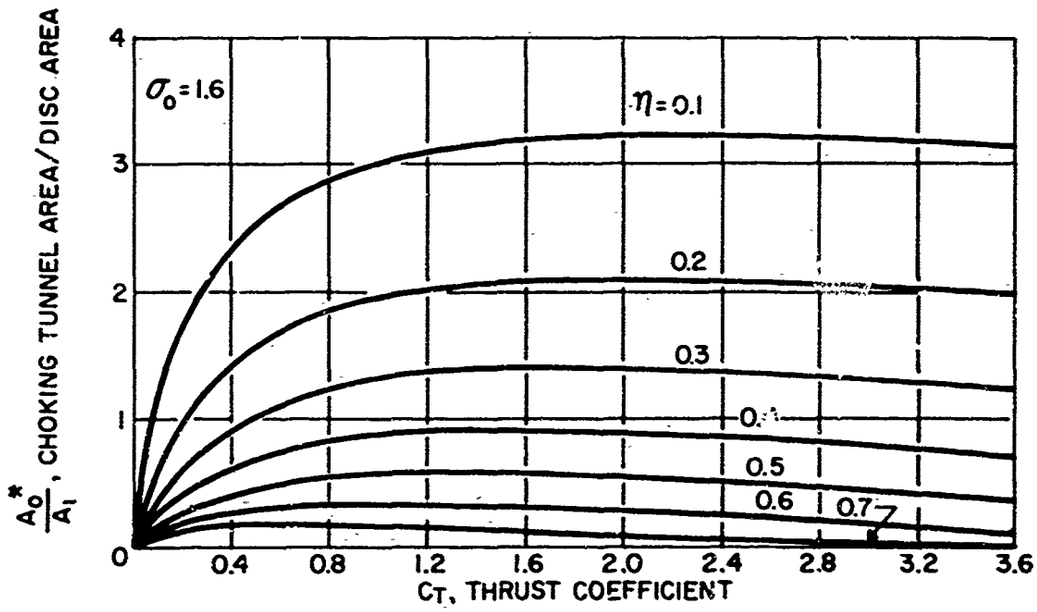

FIGURE 12e– A_0^*/A_1 VERSUS C_T , σ_0 = 1.6

UNCLASSIFIED

Security Classification

DOCUMENT CONTROL DATA - R&D

(Security classification of title, body of abstract and indexing annotation must be entered when the overall report is classified)

1. ORIGINATING ACTIVITY (Corporate author) HYDRONAUTICS, Incorporated Howard County, Pindell School Road, Laurel, Maryland	2a. REPORT SECURITY CLASSIFICATION UNCLASSIFIED 2b. GROUP

3. REPORT TITLE

SUPERCAVITATING PROPELLERS - MOMENTUM THEORY

4. DESCRIPTIVE NOTES (Type of report and inclusive dates)

Technical Report

5. AUTHOR(S) (Last name, first name, initial)

Tulin, Marshall P.

6. REPORT DATE	7a. TOTAL NO. OF PAGES	7b. NO. OF REFS
September 1964	69	19

8a. CONTRACT OR GRANT NO.	9a. ORIGINATOR'S REPORT NUMBER(S)
Nonr-3435(00) b. PROJECT NO.	Technical Report 121-4
c.	9b. OTHER REPORT NO(S) (Any other numbers that may be assigned this report)
d.	

10. AVAILABILITY/LIMITATION NOTICES

11. SUPPLEMENTARY NOTES	12. SPONSORING MILITARY ACTIVITY
	Office of Naval Research Code 438

13. ABSTRACT Based entirely on momentum and other simple considerations a reasonably complete picture of the one-dimensional pressure and velocity fields associated with heavily supercavitating propellers and drag discs has been constructed.

It is shown that the flow is very often retarded while approaching a heavily supercavitating propeller, so that the so-called ideal efficiency of such a propeller takes on values in excess of unity. The ideal efficiency actually increases with decreasing blade cavitational efficiency; however, the net efficiency at the same time decreases. This retardation causes a reduction of thrust deduction, or even a change in its sign. Charts are provided from which the inflow speed may readily be estimated.

The effect of water tunnel boundaries are discussed, particularly the phenomena of choking.

DD FORM 1 JAN 64 1473

UNCLASSIFIED

Security Classification

14. KEY WORDS	LINK A		LINK B		LINK C	
	ROLE	WT	ROLE	WT	ROLE	WT
Supercavitation Propellers Supercavitating Propellers Momentum Theory Thrust Deduction Ideal Efficiency						

INSTRUCTIONS

1. ORIGINATING ACTIVITY: Enter the name and address of the contractor, subcontractor, grantee, Department of Defense activity or other organization *(corporate author)* issuing the report.

2a. REPORT SECURITY CLASSIFICATION: Enter the overall security classification of the report. Indicate whether "Restricted Data" is included. Marking is to be in accordance with appropriate security regulations.

2b. GROUP: Automatic downgrading is specified in DoD Directive 5200.10 and Armed Forces Industrial Manual. Enter the group number. Also, when applicable, show that optional markings have been used for Group 3 and Group 4 as authorized.

3. REPORT TITLE: Enter the complete report title in all capital letters. Titles in all cases should be unclassified. If a meaningful title cannot be selected without classification, show title classification in all capitals in parenthesis immediately following the title.

4. DESCRIPTIVE NOTES: If appropriate, enter the type of report, e.g., interim, progress, summary, annual, or final. Give the inclusive dates when a specific reporting period is covered.

5. AUTHOR(S): Enter the name(s) of author(s) as shown on or in the report. Enter last name, first name, middle initial. If military, show rank and branch of service. The name of the principal author is an absolute minimum requirement.

6. REPORT DATE: Enter the date of the report as day, month, year; or month, year. If more than one date appears on the report, use date of publication.

7a. TOTAL NUMBER OF PAGES: The total page count should follow normal pagination procedures, i.e., enter the number of pages containing information.

7b. NUMBER OF REFERENCES: Enter the total number of references cited in the report.

8a. CONTRACT OR GRANT NUMBER: If appropriate, enter the applicable number of the contract or grant under which the report was written.

8b, 8c, & 8d. PROJECT NUMBER: Enter the appropriate military department identification, such as project number, subproject number, system numbers, task number, etc.

9a. ORIGINATOR'S REPORT NUMBER(S): Enter the official report number by which the document will be identified and controlled by the originating activity. This number must be unique to this report.

9b. OTHER REPORT NUMBER(S): If the report has been assigned any other report numbers *(either by the originator or by the sponsor)*, also enter this number(s).

10. AVAILABILITY/LIMITATION NOTICES: Enter any limitations on further dissemination of the report, other than those imposed by security classification, using standard statements such as:

(1) "Qualified requesters may obtain copies of this report from DDC."

(2) "Foreign announcement and dissemination of this report by DDC is not authorized."

(3) "U. S. Government agencies may obtain copies of this report directly from DDC. Other qualified DDC users shall request through _____."

(4) "U. S. military agencies may obtain copies of this report directly from DDC. Other qualified users shall request through _____."

(5) "All distribution of this report is controlled. Qualified DDC users shall request through _____."

If the report has been furnished to the Office of Technical Services, Department of Commerce, for sale to the public, indicate this fact and enter the price, if known.

11. SUPPLEMENTARY NOTES: Use for additional explanatory notes.

12. SPONSORING MILITARY ACTIVITY: Enter the name of the departmental project office or laboratory sponsoring *(paying for)* the research and development. Include address.

13. ABSTRACT: Enter an abstract giving a brief and factual summary of the document indicative of the report, even though it may also appear elsewhere in the body of the technical report. If additional space is required, a continuation sheet shall be attached.

It is highly desirable that the abstract of classified reports be unclassified. Each paragraph of the abstract shall end with an indication of the military security classification of the information in the paragraph, represented as *(TS)*, *(S)*, *(C)*, or *(U)*.

There is no limitation on the length of the abstract. However, the suggested length is from 150 to 225 words.

14. KEY WORDS: Key words are technically meaningful terms or short phrases that characterize a report and may be used as index entries for cataloging the report. Key words must be selected so that no security classification is required. Identifiers, such as equipment model designation, trade name, military project code name, geographic location, may be used as key words but will be followed by an indication of technical context. The assignment of links, roles, and weights is optional.

DISTRIBUTION LIST
(Contract Nonr-3435(00))

Chief of Naval Research
Department of the Navy
Washington 25, D. C.
Attn: Codes 438 — 3
461 — 1
463 — 1
466 — 1

Commanding Officer
Office of Naval Research
Branch Office
495 Summer Street
Boston 10, Massachusetts — 1

Commanding Officer
Office of Naval Research
Branch Office
207 West 24th Street
New York 11, New York — 1

Commanding Officer
Office of Naval Research
Branch Office
1030 East Green Street
Pasadena, California — 1

Commanding Officer
Office of Naval Research
Branch Office
1000 Geary Street
San Francisco 9, California — 1

Commanding Officer
Office of Naval Research
Branch Office
Box 39, Navy No. 100
Fleet Post Office
New York, New York — 25

Director
U. S. Naval Research Laboratory
Washington 25, D. C.
Attn: Code 2027 — 6

Chief, Bureau of Naval Weapons
Department of the Navy
Washington 25, D. C.
Attn: Codes RUTO-32 — 1
RRRE — 1
RAAD — 1
RAAD-222 — 1
DIS-42 — 1

Chief, Bureau of Ships
Department of the Navy
Washington 25, D. C.
Attn: Codes 310 — 1
312 — 1
335 — 1
420 — 1
421 — 1
440 — 1
442 — 1
449 — 1
436 — 2

Chief, Bureau of Yards and Docks
Department of the Navy
Washington 25, D. C.
Attn: Code D-400 — 1

Commander
U. S. Naval Ordnance Test Station
China Lake, California
Attn: Code 753 — 1

Commanding Officer and Director
David Taylor Model Basin
Washington 7, D. C.
Attn: Codes 108 1
142 1
500 1
513 1
520 1
525 1
526 1
526A 1
530 1
533 1
580 1
585 1
589 1
591 1
591A 1
700 1

Commander
U. S. Naval Ordnance Test Station
Pasadena Annex
3202 E. Foothill Blvd.
Pasadean 8, California
Attn: Code P-508 1

Commander
Planning Department
Portsmouth Naval Shipyard
Portsmouth, New Hampshire 1

Commander
Planning Department
Boston Naval Shipyard
Boston 29, Massachusetts 1

Commander
Planning Department
Pearl Harbor Naval Shipyard
Navy No. 128, Fleet Post Office
San Francisco, California 1

Commander
Planning Department
San Francisco Naval Shipyard
San Francisco 24, California 1

Shipyard Technical Library
Code 303TL, Bldg. 746
Mare Island Naval Shipyard
Vallejo, California 1

Commander
Planning Department
New York Naval Shipyard
Brooklyn 1, New York 1

Commander
Planning Department
Puget Sound Naval Shipyard
Bremerton, Washington 1

Commander
Planning Department
Philadelphia Naval Shipyard
U. S. Naval Base
Philadelphia 12, Pennsylvania 1

Commander
Planning Department
Norfolk Naval Shipyard
Portsmouth, Virginia 1

Commander
Planning Department
Charleston Naval Shipyard
U. S. Naval Base
Charleston, South Carolina 1

Commander
Planning Department
Long Beach Naval Shipyard
Long Beach 2, California 1

Commander
Planning Department
U. S. Naval Weapons Laboratory
Dahlgren, Virginia 1

Commander
U. S. Naval Ordnance Laboratory
White Oak, Maryland 1

Dr. A. V. Hershey
Computation and Exterior
Ballistics Laboratory
U. S. Naval Weapons Laboratory
Dahlgren, Virginia 1

Superintendent
U. S. Naval Academy
Annapolis, Maryland
Attn: Library 1

Superintendent
U. S. Naval Postgraduate School
Monterey, California 1

Commandant
U. S. Coast Guard
1300 E. Street, N. W.
Washington, D. C. 1

Secretary Ship Structure
Committee
U. S. Coast Guard Headquarters
1300 E. Street, N. W.
Washington, D. C. 1

Commander
Military Sea Trans. Service
Department of the Navy
Washington 25, D. C. 1

U. S. Maritime Administration
GAO Building
441 G. Street, N. W.
Washington, D. C.
Attn: Div. of Ship Design 1
Div. of Research 1

Superintendent
U. S. Merchant Marine Academy
Kings Point, Long Island,
New York
Attn: CAPT L. S. McCready
(Dept. of Engr.) 1

Commanding Officer and Director
U. S. Navy Mine Defense Lab.
Panama City, Florida 1

Commanding Officer
NROTC and Naval Adm. Unit
Massachusetts Institute of
Technology
Cambridge 39, Massachusetts 1

U. S. Army Transportation
Research and Dev. Command
Fort Eustis, Virginia
Attn: Marine Transport Div. 1

Mr. J. B. Parkinson
National Aeronautics and
Space Administration
1512 H. Street, N. W.
Washington 25, D. C. 1

Director
Langley Research Center
Langley Station
Hampton, Virginia
Attn: Mr. I.E. Garrick 1
Mr. D.J. Marten 1

Director
Engineering Sciences Division
National Science Foundation
1951 Constitution Ave., N. W.
Washington 25, D. C. 1

Director
National Bureau of Standards
Washington 25, D. C.
Attn: Fluid Mechanics Division
(Dr. G.B. Schubauer) 1
Dr. G.H. Keulegan 1
Dr. J.M. Franklin 1

Defense Documentation Center
Cameron Station
Alexandria, Virginia 20

Office of Technical Services
Department of Commerce
Washington 25, D. C. 1

California Institute of
Technology
Pasadena 4, California
Attn: Professor M.S. Plesset 1
Professor T. Y. Wu 1
Professor A.J. Acosta 1

University of California
Department of Engineering
Los Angeles 24, California
Attn: Dr. A. Powell 1

Director
Scripps Institute of Oceanography
University of California
La Jolla, California 1

Professor M. L. Albertson
Department of Civil Engineering
Colorado A and M College
Fort Collins, Colorado 1

Professor J. E. Cermak
Department of Civil Engineering
Colorado State University
Fort Collins, Colorado 1

Professor W. R. Sears
Graduate School or Aeronautical
Engineering
Cornell University
Ithaca, New York 1

State University of Iowa
Iowa Institute of Hydraulic
Research
Iowa City, Iowa
Attn: Dr. H. Rouse 1
Dr. L. Landweber 1

Harvard University
Cambridge 38, Massachusetts
Attn: Professor G. Birkhoff
(Dept. of Mathematics) 1
Professor G.F. Carrier
(Dept. of Mathematics) 1

Massachusetts Institute of
Technology
Cambridge 39, Massachusetts
Attn: Professor A.T. Ippen
(Dept of Naval Arch.
and Marine Engr.) 1

University of Michigan
Ann Arbor, Michigan
Attn: Professor R.B. Couch
(Dept. of Naval Arch.) 1
Professor W.W. Willmarth
(Aero Engr. Dept.) 1

Dr. L. G. Straub, Director
St. Anthony Falls Hydraulic Lab.
University of Minnesota
Minneapolis 14, Minnesota 1
Attn: Mr. J.N. Wetzel 1
Professor B.Silberman 1

Professor J. J. Foody
Engineering Department
New York State University
Maritime College
Fort Schulyer, New York 1

New York University
Institute of Mathematical
Sciences
25 Waverly Place
New York 3, New York
Attn: Professor J. Keller 1
Professor J.J. Stoker 1

The Johns Hopkins University
Department of Mechanical Engr.
Baltimore 18, Maryland
Attn: Professor S. Corrsin 1
Professor O.M. Phillips 2

Massachusetts Institute of Tech.
Department of Naval Archi-
tecture and Marine Engr.
Cambridge 39, Massachusetts
Attn: Prof. M.A.Abkowitz 1

Dr. G. F. Wislicenus
Ordnance Research Laboratory
Pennsylvania State University
University Park, Pennsylvania 1
Attn: Dr. M. Sevik 1

Professor R. C. DiPrima
Department of Mathematics
Rensselaer Polytechnic Institute
Troy, New York 1

Stevens Institute of Technology
Davidson Laboratory
Castle Point Station
Hoboken, New Jersey
Attn: Mr. D. Savitsky 1
Mr. J. P. Breslin 1
Mr. C. J. Henry 1
Mr. S. Tsakonas 1

Webb Institute of Naval
Architecture
Crescent Beach Road
Glen Cove, New York
Attn: Professor E.V. Lewis 1
Technical Library 1

Director
Woods Hole Oceanographic Inst.
Woods Hole, Massachusetts 1

Executive Director
Air Force Office of
Scientific Research
Washington 25, D. C.
Attn: Mechanics Branch 1

Commander
Wright Air Development Division
Aircraft Laboratory
Wright-Patterson Air Force
Base, Ohio
Attn: Mr. W. Mykytow,
Dynamics Branch 1

Cornell Aeronautical Laboratory
4455 Genesee Street
Buffalo, New York
Attn: Mr. W. Targoff 1
Mr. R. White 1

Massachusetts Institute of Tech.
Fluid Dynamics Research Lab.
Cambridge 39, Massachusetts
Attn: Professor H. Ashley 1
Professor M. Landahl 1
Professor J. Dugundji 1

Hamburgische Schiffbau-
Versuchsanstalt
Bramfelder Strasse 164
Hamburg 33, Germany
Attn: Dr. H. W. Lerbs 1

Institut fur Schiffbau der
Universitat Hamburg
Lammersieth 90
Hamburg 33, Germany
Attn: Professor O. Grim 1
Prof. K. Wieghardt 1

Transportation Technical
Research Institute
1-1057, Mejiro-Cho, Toshima-Ku
Tokyo, Japan 1

Max-Planck Institute fur
Stromungsforschung
Bottingerstrasse 6/8
Gottingen, Germany
Attn: Dr. H. Reichardt 1

Hydro-og Aerodynamisk
Laboratorium
Lyngby, Denmark
Attn: Prof. Carl Prohaska 1

Skipsmodelltanken
Trondheim, Norway
Attn: Professor J.K. Lunde 1

Versuchsanstalt fur Wasserbau
und Schiffbau
Schleuseninsel im Tiergarten
Berlin, Germany
Attn: Dr. S. Schuster, Dir. 1
Dr. Grosse 1

Technische Hogeschool
Institut voor Toegepaste
Wiskunde
Julianalaan 132
Delft, Netherlands
Attn: Professor R. Timman 1

Bureau D'Analyse et de Recherche
Appliquees
47 Avenue Victor Cresson
Issy-Les-Moulineaux
Seine, France
Attn: Professor Siestrunck 1

Netherlands Ship Model Basin
Wageningen, The Netherlands
Attn: Dr. Ir.J. D. Van Manen 1

National Physical Laboratory
Teddington, Middlesex, England
Attn: Mr. A. Silverleaf,
Superintendent Ship Div. 1
Head, Aerodynamics Div. 1

Head, Aerodynamics Department
Royal Aircraft Establishment
Farnborough, Hants, England
Attn: Mr. M.O.W. Wolfe 2

Dr. S. F. Hoerner
148 Busteed Drive
Midland Park, New Jersey 1

Boeing Airplane Company
Seattle Division
Seattle, Washington
Attn: Mr. M.J. Turner 1

Electric Boat Division
General Dynamics Corporation
Groton, Connecticut
Attn: Mr. Robert McCandliss 1

General Applied Sciences Lab., Inc.
Merrick and Stewart Avenues
Westbury, Long Island, N.Y. 1

Gibbs and Cox, Inc.
21 West Street
New York, New York 1

Grumman Aircraft Engineering Corporation, Bethpage, Long Island, New York
Attn: Mr. E. Baird 1
Mr. E. Bower 1
Mr. W. P. Carl 1

Lockheed Aircraft Corporation
Missiles and Space Division
Palo Alto, California
Attn: R. W. Kermeen 1

Midwest Research Institute
425 Voker Blvd.
Kansas City 10, Missouri
Attn: Mr. Zeydel 1

Director, Department of Mechanical Sciences
Southwest Research Institute
8500 Culebra Road
San Antonio 6, Texas
Attn: Dr. H.N. Abramson 1
Mr. G. Ransleben 1
Editor, Applied Mechanics Review 1

Convair
A Division of General Dynamics
San Diego, California
Attn: Mr. R.H. Oversmith 1
Mr. H.T. Brooke 1

Hughes Tool Company
Aircraft Division
Culver City, California
Attn: Mr. M.S. Harned 1

HYDRONAUTICS, Incorporated
Pindell School Road
Howard County
Laurel, Maryland
Attn: Mr. Phillip Eisenberg 1

Rand Development Corporation
13600 Deise Avenue
Cleveland 10, Ohio
Attn: Dr. A.S. Iberall 1

U. S. Rubber Company
Research and Development Dept.
Wayne, New Jersey
Attn: Mr. L.M. White 1

Technical Research Group, Inc.
Route 110
Melville, New York
Attn: Dr. Jack Kotik 1

Mr. C. Wigley
Flat 102
6-9 Charterhouse Square
London, E.C. 1, England 1

AVCO Corporation
Lycoming Division
1701 K. Street, N. W.
Apt. 904
Washington, D. C.
Attn: Mr. T.A. Duncan 1

Mr. J. G. Baker
Baker Manufacturing Company
Evansville, Wisconsin 1

Curtis-Wright Corporation
Research Division
Turbomachinery Division
Quehanna, Pennsylvania
Attn: Mr. George H. Pedersen 1

Dr. Blaine R. Parkin
AiResearch Manufacturing Corp.
9851-9951 Sepulveda Boulevard
Los Angeles 45, California 1

The Boeing Company
Aero-Space Division
Seattle 24, Washington
Attn: Mr. R.E. Bateman
(Internal Mail Station
46-74) 1

Lockheed Aircraft Corporation
California Division
Hydrodynamics Research
Burbank, California
Attn: Mr. Bill East 1

National Research Council
Montreal Road
Ottawa 2, Canada
Attn: Mr. E.S. Turner 1

The Rand Corporation
1700 Main Street
Santa Monica, California
Attn: Technical Library 1

Stanford University
Department of Civil Engineering
Stanford, California
Attn: Dr. Byrne Perry 1
Dr. E. Y. Hsu 1

Dr. Hirsh Cohen
IBM Research Center
P. O. Box 218
Yorktown Heights, New York 1

Mr. David Wellinger
Hydrofoil Projects
Radio Corporation of America
Burlington, Massachusetts 1

Food Machinery Corporation
P. O. Box 367
San Jose, California
Attn: Mr. G. Tedrew 1

Dr. T. R. Goodman
Oceanics, Incorporated
Technical Industrial Park
Plainview, Long Island,
New York 1

Commanding Officer
Office of Naval Research
Branch Office
230 N. Michigan Avenue
Chicago 1, Illinois 1

Professor J. William Holl
Dept. of Aeronautical Engr.
The Pennsylvania State Univ.
Ordnance Research Laboratory
P. O. Box 30
State College, Pennsylvania 1

Professor Brunelle
Department of Aeronautical Engr.
Princeton University
Princeton, New Jersey 1

National Academy of Science
National Research Council
Committee on Undersea Warfare
2101 Constitution Avenue
Washington 25, D. C. 1

Dr. Harvey Brooks
School of Applied Science
Harvard University
Cambridge, Massachusetts 1